The Chemical Composition of Exoplanet-hosting Binary Star Systems

by

Bryce Carande

A Thesis Presented in Partial Fulfillment
of the Requirement for the Degree
Master of Science

Approved November 2013 by the
Graduate Supervisory Committee:

Patrick Young, Co-Chair
Jennifer Patience, Co-Chair
Ariel Anbar

ARIZONA STATE UNIVERSITY

December 2013

ABSTRACT

A significant portion of stars occur as binary systems, in which two stellar components orbit a common center of mass. As the number of known exoplanet systems continues to grow, some binary systems are now known to harbor planets around one or both stellar components. As a first look into composition of these planetary systems, I investigate the chemical compositions of 4 binary star systems, each of which is known to contain at least one planet. Stars are known to vary significantly in their composition, and their overall metallicity (represented by iron abundance, [Fe/H]) has been shown to correlate with the likelihood of hosting a planetary system. Furthermore, the detailed chemical composition of a system can give insight into the possible properties of the system's known exoplanets. Using high-resolution spectra, I quantify the abundances of up to 28 elements in each stellar component of the binary systems 16 Cyg, 83 Leo, HD 109749, and HD 195019. A direct comparison is made between each star and its binary companion to give a differential composition for each system. For each star, a comparison of elemental abundance vs. condensation temperature is made, which may be a good diagnostic of refractory-rich terrestrial planets in a system. The elemental ratios C/O and Mg/Si, crucial in determining the atmospheric composition and mineralogy of planets, are calculated and discussed for each star. Finally, the compositions and diagnostics of each binary system are discussed in terms of the known planetary and stellar parameters for each system.

Dedications:

I would like to dedicate this thesis to my loving and amazing wife, Wendy. Without her support, encouragement, and strength (from around the corner or around the world), this thesis would have been impossible.

Thank you to everyone who's helped me along the way, through all my stages of graduate school, and most especially to all of my advisors, teachers, and mentors. I have been fortunate to learn under such wise and understanding direction.

Finally, to my parents: thank you for everything, for challenging and supporting me, and for constantly pushing me to follow my interests. You've started me on this path long ago, and have been leading me forward ever since.

ACKNOWLEDGMENTS

This research has been made possible by several open-access databases and research tools. General exoplanet information was obtained from The Extrasolar Planets Encyclopedia, at www.exoplanets.eu

This research has made use of the SIMBAD database, and VizieR catalogue access tool, both operated at CDS, Strasbourg, France. The original description of the VizieR service was published in A&AS 143, 23.

This research has made use of the Keck Observatory Archive (KOA), which is operated by the W. M. Keck Observatory and the NASA Exoplanet Science Institute (NExScI), under contract with the National Aeronautics and Space Administration.

Finally, I would like to gratefully acknowledge multiple semesters of graduate RA funding for this research through NASA's Astrobiology Institute (NAI) node at ASU.

TABLE OF CONTENTS

CHAPTER Page

LIST OF TABLES

LIST OF FIGURES

Figure Page

Figure Page

Chapter 1

INTRODUCTION

1.1 Discovery of exoplanets

In a time span of less than 2 decades, the study of extrasolar planets (exoplanets) has progressed at a rapid rate. According to the Extrasolar Planets Encyclopaedia (exoplanets.eu, as of November 2013), there are currently 1039 known exoplanets, composing 787 planetary systems. There have been several methods developed to detect these exoplanets, each method providing different types of information regarding the planetary systems (Perryman, 2011). Three of the primary detection methods (radial velocity, transit, and direct imaging) are discussed here, although additional methods (such as gravitational lensing) also exist.

The first method used to detect exoplanets involves measuring the reflex motion of the host star caused by the gravitational pull of an orbiting planetary companion (Hatzes *et al.*, 2010). The radial component of this induced motion causes an observed Doppler shift of the star's spectrum. This method, known as Radial Velocity (RV) detection, requires a high-resolution spectrum of the star's light in order to resolve the small Doppler shift caused by the star's planet(s). These data allow the determination of a planet's orbital period and the in-plane mass, or $M*Sin(i)$- a more massive planet on a more inclined orbit could cause the same radial velocity signal.

Transit Photometry, another very successful exoplanet detection method, relies on the slight reduction of observed light from a star when a planet passes in front of the star's surface (Bord *et al.* (2003), Borucki *et al.* (2009)). This results in an estimate of the planet's size (as compared to the host star), as well as the orbital period.

Transit detections are inherently limited to systems with near-zero inclinations - the system must be close to edge-on for the transit to be observable from Earth. Transit and RV measurements provide complimentary knowledge about a system, together yielding both mass and size information about a planet, allowing its density to also be constrained (Moutou *et al.*, 2004).

For nearby exoplanet systems with young giant planets at large orbital distances, direct imaging has also become a method to detect and study exoplanets. Recent advances in Adaptive Optics (AO) have allowed for sub-arcsecond resolution, allowing thermal emission from giant planets to be directly observable (Patience *et al.* (2002), Rameau *et al.* (2013)).

Beyond simply detecting the size, mass, and orbital properties of exoplanets, their atmospheric and bulk compositions can also be inferred by combining spectroscopy techniques with the methods described above. Spectral analysis of directly imaged planets has been used to deduce their atmospheric composition (Oppenheimer *et al.*, 2013). Spectroscopy of a host star during a known planetary transit can probe the composition and scale height of the planetary atmosphere.

1.2 Host star composition

Although direct imaging spectroscopy and transit spectroscopy can produce impressive results, they are only applicable to a small subset of known systems, relying on minimum orbital separation and planet brightness (in the case of direct imaging), and fortunate orbital alignment to allow for observable transits (in the case of transit spectroscopy). By contrast, high-resolution spectroscopy of a system's host star is widely applicable, and can yield detailed elemental composition of the host star. This method relies on measuring the strength of elemental absorption features present in a star's spectra, so the spectral data must be of sufficiently high resolution and

signal-to-noise to resolve these absorption features. RV measurements require high-resolution spectra for the initial exoplanet discoveries, so high-resolution datasets (of appropriate quality for this analysis) already exist for many known planetary systems. Therefore, this method provides a simple and widely-applicable first look at the overall composition of an exoplanetary system.

This method has been used to study the composition of many exoplanet host stars, however few studies have focused exclusively on host stars in binary or multiple systems. The goal of this research is to use existing high-resolution spectra to measure the composition of each stellar component of several binary systems known to contain exoplanets. This will allow the compositions of those individual planetary systems to be constrained, as well as giving clues about the long-term history of the planetary and stellar systems. Furthermore, a comparison between binary components will be made to look for any systematic differences between binary partners having planets, and those without currently known planets. Binary systems are an ideal comparison because the stars are very likely to have formed from the same protostellar nebula at nearly the same time, giving them very similar ages and initial compositions.

Deriving abundances for elements in stars can be done in a variety of ways. One of the more detailed ways, which is employed in this study, involves measuring the strength of individual atomic absorption lines in a high-resolution stellar spectrum, and then employing a spectral synthesis program such as MOOG and a model stellar atmosphere to determine what the abundance of each elemental species must be. A more detailed description of this process is given in Chapter 2.

1.2.1 Reliability of composition studies

Derivations of astrophysical abundances have long been questioned regarding their degree of accuracy (Worrall, 1972). The abundance analysis method is sensitive to

several choices in methodology, and groups with different methodologies may derive discrepant results, even if they use the same input data (Asplund, 2005). The stellar parameters used to generate a model atmosphere can be derived in several ways; the choice of how these parameters are picked will certainly affect the results. Furthermore, the choice of which lines to measure for each element (i.e. the linelist) can have an effect on the derived abundance. Typically, measuring more lines will produce a more robust result, but only if the lines are accurately measured and if line blending is properly accounted for. Line blending occurs when two absorption features are partially overlapping each other, causing what may appear to be a single, larger absorption feature. For an accurate measurement, only the contribution from the line corresponding to the element of interest must be measured. Also, the continuum for a star must be properly normalized around a line before it can be accurately measured.

The assumption of a specific solar composition is included in a reported stellar abundance. Adopting different solar abundances can be a source of error between different groups. Furthermore, some groups will derive overall abundances for each element, and compare those results with reported solar values. Other groups, to compensate for instrumental effects, will compare abundances line-by-line with a measured solar spectrum, without using published solar abundances.

Therefore, studies employing a single methodology across multiple stars may produce more meaningful results than a comparison of results from separate groups with different methods. For the most accurate comparison of stellar compositions, identical methodologies -such as from a single study- must be used. Even if the absolute abundances from a single study are proven to be incorrect, the relative abundances between stars in that study should still be comparable.

1.3 Formation and composition of planetary systems

Stellar composition can provide valuable insights about a planetary system, even if it does not directly reveal planetary composition. Stars compose the vast majority of the mass in planetary systems, and therefore give a good overall indication of the system's composition. In turn, system composition can help answer questions related to how planets form, and what those planets are likely made of. Furthermore, stellar composition can place some constraints on the long-term history of a system. A star's overall luminosity and evolutionary speed are affected by its composition (particularly oxygen and iron-peak elements), which can have drastic effects on the location and duration of its habitable zone (Young *et al.*, 2012). Furthermore, a star's photospheric composition may preserve traces of planetary accretion events that have happened in the system's past.

Planets form out of condensed material in the protoplanetary disc, so the composition of the primordial material making up this disc determines the resulting composition of the newly formed planets. A star contains the vast majority of the mass in a stellar system, and the resulting stellar composition will not change drastically from the primordial molecular cloud core or protoplanetary disc composition. Gravitational settling and mixing will affect the composition of the stellar atmosphere (as compared to the star's bulk composition), in a way that can be incorporated into models. A system's refractory elements may be preferentially sequestered in planets, which could also be re-accreted on the star. Overall, however, these are likely small perturbations on the initial abundances, and the stellar atmosphere does provide a representative composition of the overall system (Santos *et al.* (2001), Santos *et al.* (2003), Fischer and Valenti (2005)). This composition can be used to understand the early history and formation process of a stellar system, including the metallicity

and heavy element enrichment of the original molecular cloud, as well as subsequent enrichment such as injections of supernovae material.

1.3.1 Planet-metallicity correlations

One of the early discoveries regarding the statistics of exoplanet host star composition was the Planet-Metallicity correlation (Fischer and Valenti (2005), Santos *et al.* (2005)). These studies established a positive correlation between Iron abundance (Fe/H) and planet frequency in a sample of F,G, and K type RV host stars. This planet-metallicity correlation has also been found to hold for other stellar types, being extended to M stars in the solar neighborhood by Johnson and Apps (2009). The planet-metallicity trend has been found to be more significant for higher-mass planets Guillot *et al.* (2006), with a weaker correlation for sub-Neptune and super-Earth sized planets.

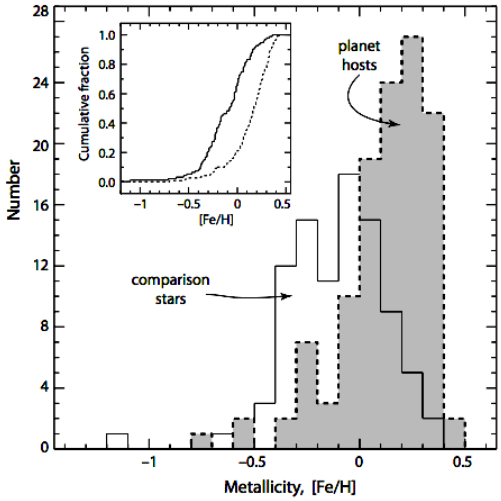

Figure 1.1: A histogram comparing the metallicities of planet-host and non-host stellar populations. Figure reproduced from Figure 1 of Santos *et al.* (2005)

1.3.2 Formation mechanisms

For giant planets, the two main formation hypotheses are by gravitational instabilities or by core accretion. The gravitational instability model (Boss (1997) and Boss (2011)) describes the direct self-gravitating fragmentation of a protoplanetary disc into protoplanetary clouds, which can then condense into giant planets. The effectiveness of this formation mechanism depends primarily on the mass density and mass profile of the protoplanetary disc, and is not significantly influenced by disc composition.

In the core accretion models (Matsuo *et al.* (2007), Mordasini *et al.* (2007), Ida and Lin (2004)), solid materials condense from the protoplanetary disc as it cools. These solid materials form protoplanets, which collide and build until they are big enough to grow via gravitational attraction of other material. If the resulting planet embryo can form before the gaseous material has dissipated from the protoplanetary disc, then the planet will acquire a gaseous envelope. Because gas dissipates from the disc over time, the faster a planetary embryo can form (and the more massive it is), the more gas will be available to that planet, and the larger its overall mass will be (Kokubo and Ida (2002), Rice *et al.* (2012)).

Composition can effect the speed and efficiency of core formation, and thus the type of resulting planets. In a system with higher metallicity, a larger proportion of the materials will be in the form of early-condensing metallic elements (such as iron), allowing planetary embryos to form more rapidly and grow larger. Furthermore, in outer regions of the protoplanetary disc, volatiles such as C and O form into ices, so a higher abundance of these elements will give additional material to protoplanets forming in these regions (Öberg *et al.*, 2011). Because of this, the planet-metallicity

correlation of Fischer and Valenti (2005) gives strong observational support to the core accretion modes of planetary formation.

1.3.3 Effects of composition

A system's composition, especially in the abundance ratios of certain elements, can have many effects on both the star(s) and planets in that system - including effects related to habitability. Stellar composition affects a star's emergent properties (such as effective temperature and luminosity), as well as its long-term evolution. Both of these effects play an important role in the location and lifetime of a star's habitable zone. Oxygen abundance has been found to be particularly important in the lifetime of a star's habitable zone, potentially changing the duration of a habitable zone by gigayears at a given orbital distance (Young *et al.*, 2012).

The physical properties of planets in a system will be strongly influenced by the abundance ratios of key elements, particularly elements with important roles in rock and mineral formation, such as C, O, Si, Fe, and Mg. The C/O ratio is of particular importance for planetary formation and composition (Öberg *et al.*, 2011), affecting condensation pathways (Bond *et al.*, 2010), determining whether rocky planets will be dominated by silicate or carbide chemistry, and affecting the atmospheric chemistry of giant planets (Madhusudhan *et al.*, 2011). In terrestrial silicate planets such as the Earth, the Mg/Si ratio sets the mineralogy of the mantle, particularly the relative abundances of the dominant minerals Olivine and Pyroxene (Bond *et al.*, 2010). Variations in this mantle composition have strong effects on mantle structure and dynamics (Ammann *et al.* (2011), de Koker *et al.* (2013)), particularly convection processes, which could potentially influence plate tectonic activity. Finally, the Fe/Si ratio will manifest in terrestrial planets as the relative size of the iron core to the rocky silicon-rich mantle.

1.4 Binary Systems

Studies of stellar multiplicity among G and K type stars in the solar neighborhood have shown that the majority of these stars (over 60%) occur in binary or multiple systems (Eggenberger *et al.* (2004), Duquennoy and Mayor (1991)). Because multiple systems are so common, they represent an important component in understanding the overall processes of star and planet formation and dynamics.

In these systems, any compositional differences between components is often of great interest, requiring studies with consistent methodology. Composition studies of wide-separation binaries provide a unique, extremely localized probe of planet-forming conditions. Wide-separation binaries typically experience coeval formation, from the same nebular material, usually separated by between 1,000 to 10,000 AU. Therefore, composition studies of wide-binaries probe the differences in primordial nebular composition on a thousand-AU scale. On such a small interstellar scale, large composition differences are unlikely; any chemical enrichment event effecting one star would likely effect the other as well.

1.4.1 Exoplanets in Binary Systems

Exoplanets in binary systems can orbit a single star of the pair (an S-type orbit), or can posses and orbit encircling both stellar components (a P-type orbit) (Haghighipour *et al.*, 2009). P-type orbits are much less common, and are more likely to occur around very close binaries. Also, P-type orbits imply a different and possibly more complex formation and evolution as compared to planets with S-type orbits. This study is only concerned with the more common S-type orbits.

In a binary system, the same models for planetary formation still apply, but the gravitational perturbations caused by the companion star produces an effect on the

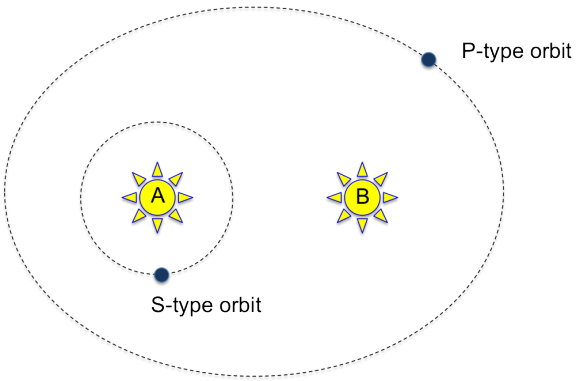

Figure 1.2: A diagram showing the S-type (orbits one component) and P-type (orbits both component) orbital configurations for an exoplanet in a binary star system.

newly-forming planets. Models indicate that in binary systems, a dust disc will be truncated, and the condensed materials will fragment into smaller particles, impeding planet formation (Zsom *et al.*, 2011). The effect of disc truncation is strongly separation dependent (Duchene (2010), Desidera and Barbieri (2007)), being of little significance for wide-separation binaries.

The presence of a companion star also has a strong impact on planetary orbits (Kaib *et al.*, 2013), with planets in binary systems being much more likely to get ejected, and generally having more eccentric orbits. Desidera and Barbieri (2007) find that among known exoplanet-hosting multiple systems, giant close-in planets are common in close-separation binaries (confirming earlier statistics by Eggenberger *et al.* (2004)), but that wide binary systems have planetary systems generally similar to field stars, albeit with slightly higher average eccentricities.

Roell *et al.* (2012) performed an updated statistical study using more recently available data, and confirmed two trends in close binaries: planetary masses decrease, and planetary orbital radii increase, with increasing binary separation. This study also includes up-to-date tables of known binary systems hosting exoplanets having S-type orbits.

The search for new binary (or multiple) systems containing exoplanets can be approached in several ways, as reviewed by Muterspaugh *et al.* (2007). Planet-search surveys of known binary systems can discover new exoplanets and provide statistics on the entire population of binary host-stars. Examples of planet search surveys focused on binary systems include SARG (Gratton *et al.* (2003), Carolo *et al.* (2011)), as well as several using HARPS (Konacki (2005) and others).

Another approach is to look for undiscovered stellar companions of known exoplanet hosts. For close or dim companions, this typically requires adaptive optics imaging. Examples of searches for undiscovered stellar companions to host stars include Patience *et al.* (2002), Chauvin *et al.* (2006), Raghavan *et al.* (2006), and Mugrauer *et al.* (2006). For bright, wide separation companions, searching archival images and catalogs for co-moving objects can be sufficient. The work presented here is limited to multiples currently known in existing catalogs such as the CCDM.

1.4.2 Systems in this study

Four stellar systems have been selected for a detailed abundance analysis in this study: 16 Cygni, 83 Leonis, HD109749, and HD195019. Each system consists of at least two stellar members of spectral type G or K, with one star harboring at least one confirmed exoplanet. All systems listed here are listed as binary systems and confirmed to be physical in Roell *et al.* (2012) and/or Raghavan *et al.* (2006). The selection process used to determine these targets is explained in Chapter 2. For each system, a simplified schematic shows all currently known stellar and planetary components of the system, including separation distances.

16 Cyg (HD 186408 and HD 186427)

16 Cyg is a well-studied system consisting of a pair of solar-twin stars, each having a small companion of its own. The two main components A and B are of similar masses, and have spectral types of G1.5V and G3V. They are separated by 859.7 AU. 16 Cyg B is a known planet host, with the radial-velocity (RV) detection of 16 Cyg B b by Cochran *et al.* (1996) and confirmed by Raghavan *et al.* (2006). This planet has a $Msin(i)$ = 1.5 Mj, a semi-major axis of 1.68 AU, and a high eccentricity of e = 0.63. 16 Cyg A has also been monitored for RV signals for over 15 years, but no planets have been detected (Wittenmyer *et al.*, 2006). This non-detection excludes possible companions with $Msin(i)$ = 2.45 Mj at 5.2 AU, and smaller planets interior to this. 16 Cyg A was discovered to have an M dwarf companion though AO direct imaging (Hauser and Marcy (1999), Turner *et al.* (2001)), which is likely a physically associated binary (Patience *et al.*, 2002).

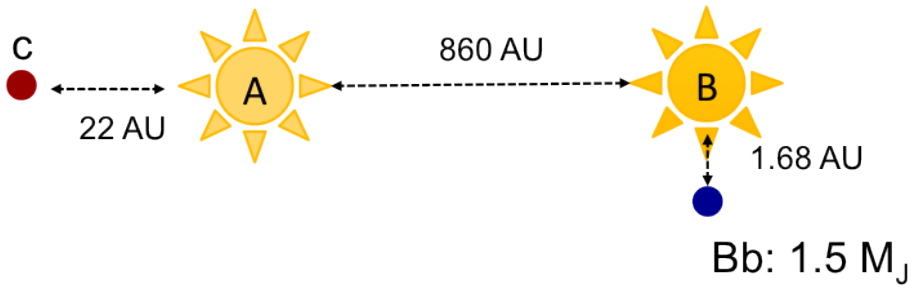

Figure 1.3: Schematic of components in the triple system 16 Cyg

83 Leo (HD 99491 and HD 99492)

83 Leo A and B are a pair of comoving high proper-motion stars, separated by 589.4 AU, with spectral types K0IV and K2V, respectively. Both stars are known to be very metal-rich, with reported [Fe/H] ranging from +0.22 (Feltzing and Gonzalez (2001)) to +0.40 (Heiter and Luck (2003)) for 83 Leo A, and +0.24 (Santos *et al.* (2005)) to

+0.36 (Heiter and Luck (2003)) for 83 Leo B. RV surveys detected a planet around the B component in Marcy *et al.* (2005), and an additional planet was announced in 2010 (Meschiari *et al.*, 2011). 83 Leo Bb has an $M*Sin(i)$ of 0.109 Mj (corresponding to $36M_{Earth}$), orbiting at .123 AU with an e of 0.254. Planet c was found to be more massive but still sub-Jovian, with an $M*Sin(i)$ of 0.36 Mj. It has a semi-major axis of 5.4 AU, and an eccentricity of 0.106. 7 years of HIRES observations did not detect any planetary RV signals from 83 Leo A (Marcy *et al.*, 2005).

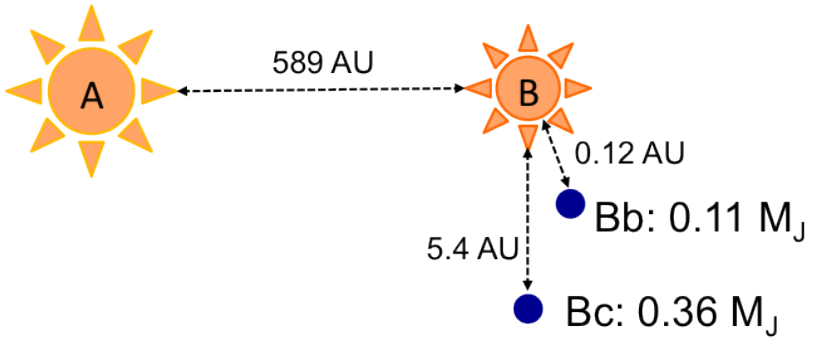

Figure 1.4: Schematic of components in the binary system 83 Leo

HD 109749

HD 109749 is a metal-rich G3 IV star at a distance of 59 pc. The two components are separated by 8.35", corresponding to 495.6 AU. A planet discovery in HD 109749 (around the A component) was reported by the N2K consortium in 2006 (Fischer *et al.*, 2006). This planet has an $M * Sin(i) = 0.28$ Mj, and orbits at a=0.06 AU. The host star was then part of a search for stellar companions to exoplanets, and a K5V companion was discovered by Desidera and Barbieri (2007) within a year.

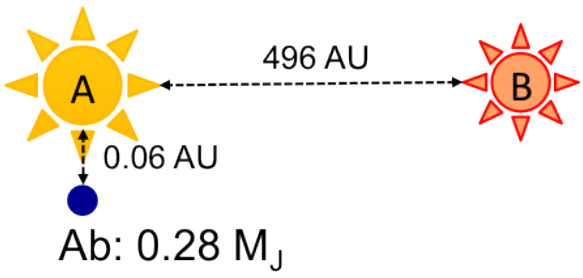

Figure 1.5: Schematic of components in the binary system HD 109749

HD 195019

The HD 195019 (also HIP 100970 or HO 131 A/B) system has long been known as a double system, first reported by Hough (1887). The primary, a G3 IV-V, was discovered to host a planet by Fischer *et al.* (1999). The planet has an $M * Sin(i)$ of 3.70 Mj, and orbits the A component at 0.14 AU. The secondary is of spectral type K3, separated at 149.2 AU. This system was listed as a wide binary in Allen *et al.* (2000) and Eggenberger *et al.* (2004). Han *et al.* (2001) also provided updated astrometry about this system.

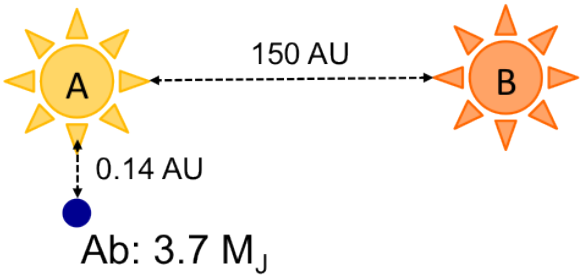

Figure 1.6: Schematic of components in the binary system HD 195019

Chapter 2

ANALYSIS AND RESULTS

In this chapter, I discuss the selection of the stellar sample, and the analysis steps taken for each star to derive elemental abundances. I present the resulting abundance measurements for each star, as well as their respective uncertainties, and compare these results to previously published studies where possible.

2.1 Method

2.1.1 Selection process

This study began by identifying stellar systems containing multiple stellar components, at least one of which is a known exoplanet host. An up-to-date list of exoplanet host stars was generated from the Extrasolar Planet Encyclopedia *(exoplanet.eu)*. Several host stars in this list were listed as being part of known multiple stellar systems in the Catalog of Components of Doubles and Multiples (CCDM). Since this catalog contains visual doubles (not physically associated) as well as true (gravitationally bound) binaries and multiples, the proper motions and parallaxes of components in each system were obtained using SIMBAD. Systems with discrepant proper motions or parallaxes were rejected, as these stars are not physically associated with each other.

In this study, only systems with both companions being F, G, or K spectral types were considered. Hotter stars (O, B, and A) are too numerically few to have resulted in matches in the present study. Furthermore, hotter stars are more difficult to analyze due to less absorption in their atmospheres. Stars cooler than K-type have

the opposite problem, becoming increasingly difficult due to crowding of the spectrum with molecular absorption features.

Due to the scope of this project, no new observations could be obtained, and this study was limited to using existing archival data. Deriving elemental abundances for a star relies on quantifying elemental absorption features, requiring a high-resolution spectrum (typically in the optical range). For this study, data from the HIRES (HIgh-RESolution Echelle Spectrograph) on Keck were used. Availability of HIRES data for both components further constrained the list of usable stellar systems, yielding a final sample of 4 multiple-component, exoplanet hosting systems for analysis: 16 Cygni, 83 Leonis, HD109749, and HD195019. Basic info on each of these systems is shown in Table 2.1.

Two additional systems were initially considered for this study, but could not be used due to observational issues. HD178911 is a system with A and B components; HD178911 B is a known planet host (Raghavan *et al.*, 2006). However, the A component is itself a spectroscopic binary (Roell *et al.*, 2012), making an accurate abundance analysis beyond the scope of this project. GJ738 is a narrow binary system, with an astrometry-detected exoplanet (Muterspaugh *et al.*, 2010) around one of the components. HIRES data are available for GJ738 A/B, but the components are unresolved, precluding abundance analysis of each star individually.

HIRES instrumental background

Although not designed as a planet-finding instrument, HIRES (Vogt *et al.*, 1994) has seen vast success in providing high-resolution spectra for the RV detection of exoplanets. Located on Keck I, HIRES is a cross-dispersed echelle sptectrograph covering the 3000 Å- 10000 Å wavelength range. Depending on the mode of operation, the spectral resolution obtainable by HIRES ranges from R = 25,000 to 85,000. HIRES

Table 2.1: Sample of 8 stars for this study

Name	HD number	Location	Proper Motion (mas/yr)	Sp. Type	Planets
16 Cyg A	186408	295.45, 50.53	-147.82, -159.01	G1.5Vb	-
16 Cyg B	186427	295.47, 50.52	-135.11, -163.78	G3V	1
-	109749 A	189.32, -40.81	-157.85, -5.43	G3V	1
-	109749 B	189.32, -40.82	-175, -43	K5V	-
HO 131A	195019 A	307.08, 18.77	348.48, -58.39	G1V	1
HO 131B	195019 B	307.08, 18.77	350.2, -58.3	K3	-
83 Leo A	99491	171.69, 3.01	-725.74, 180.67	KOIV	-
83 Leo B	99492	171.69, 3.01	-730.81, 188.97	K2V	2

originally functioned with a detector setup consisting of a single CCD; in 2002 this was replaced by a 3-ccd mosaic, to increase usable spectral resolution and sensitivity. An example of the raw flux data recorded by a single CCD for one of the analyzed stars is shown in Figure 2.1. This image shows the dispersed spectrum: light from the star is dispersed by wavelength into many long vertical lines. In each vertical line (known as a spectral order), the wavelength increases from bottom to top, and each vertical line covers a slightly different wavelength range.

Data from HIRES observations are publicly available after a proprietary period through the Keck Online Archive (KOA) system. Data for all stars in this study were downloaded using this system, making use of the built-in MAKEE pipeline for automated data reduction of the raw spectra, including flat-fielding and bias corrections. The MAKEE pipeline produces a collection of files with usable data (such as flux) split across many spectral orders. The exact number of spectral orders

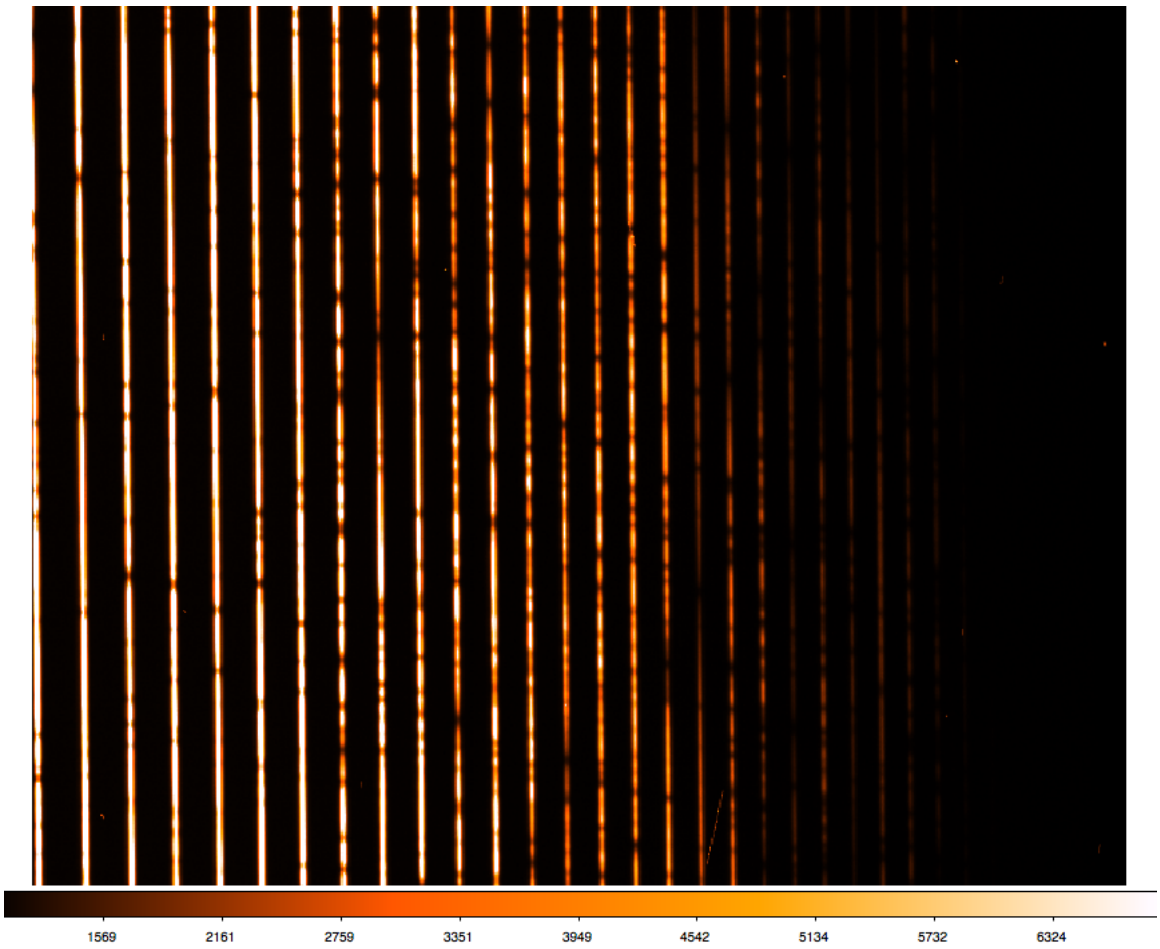

Figure 2.1: A portion of the raw flux data for 83 Leo B. The individual spectral orders are seen here as bright vertical lines.

depends on the configuration of the spectrograph during the observation. Table 2.2 gives info on each HIRES observation used for data in this study.

2.1.2 Pre-Processing

Several IDL routines and shell scripts were implemented to further process these data into a format usable by the analysis programs. The spectral dispersion (separation in wavelength between consecutive flux points) varies both within individual spectral orders, as well as from one order to the next. Because the analysis tools (*IRAF splot* and *ARES*) require a single dispersion value for computations, the flux

data needed to be converted to a single-dispersion format. To achieve this, the flux data were interpolated to a constant wavelength spacing. A Gaussian with FWHM matching the desired spectral dispersion was used to smooth the high-resolution spectrum before resampling. This ensured a single dispersion value for each spectral order. This process was written in IDL and applied to each spectral order individually.

Due to the relative radial motion of each star compared to the Earth, a Doppler shift is present in each spectrum. This shift is not corrected by the KOA *MAKEE* pipeline. Due to the Doppler shift, the observed location of spectral lines is slightly different than the "expected" (rest frame) location of those lines (as seen in Fig. 2.2). In fact, this offset is the measured quantity to precisely determine the radial velocity of stars in order to detect the presence of Exoplanets using the RV detection method. In this study, the Doppler-shift was measured using the positions of several easily-identifiable spectral lines, and comparing to the corresponding rest-frame line centers. Spectral lines in many different orders were measured, allowing a linear, wavelength-dependent Doppler shift function to be fit and applied to each stellar spectrum, order by order.

2.1.3 Linelist

The abundance of each elemental species is derived based on absorption features (as explained above). A single absorption line can be sufficient to derive an elemental abundance, however using many lines for a single element generally leads to a better result. Using multiple lines also allows a better constraint on the uncertainty in derived abundance. The linelist for this study includes 217 atomic absorption lines, from 28 elements. For comparison, similar studies have measured 24 elements (Ramírez *et al.*, 2011), 18 elements (Schuler *et al.* (2011b), Ecuvillon *et al.* (2006a)), 17 elements (Gonzalez (1998)), 12 elements (Kang *et al.*, 2011), and 9 elements (Bodaghee *et al.*,

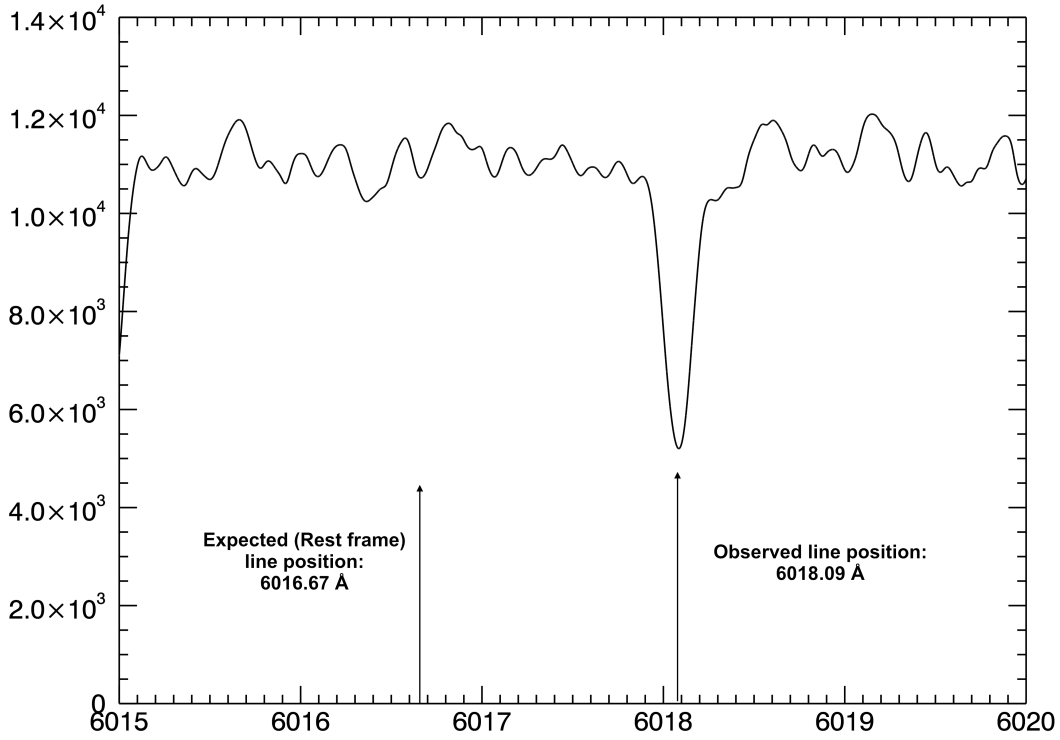

Figure 2.2: Example spectrum showing RV shift of a single line

2003). Several parameters for each line are needed, including the rest-frame line center wavelength, excitation potential, and oscillator strength. The appendix A1 shows these values for the entire line list used in this study, including the equivalent width for each line as seen in a solar spectrum. Because iron lines are used to calibrate the appropriate stellar parameters, it is important to include as many reliable iron lines as possible. This study uses 72 Fe I (neutral iron) and 16 FeII (singly-ionized iron) lines.

Some elements, such as oxygen, are particularly sensitive to line choice and methodology. Of the 5 oxygen lines used in this study, the 6155Å line is the most robust, while the 6363Å line is blended with a Ni feature. The oxygen infrared triplet consists

Table 2.2: Observations providing data for this study. The KOAID is formatted to include the observation date, as: HI.*YYYYMMDD.xxxxx*

Star Name	KOA Name	KOA ID	Spectral Coverage (Å)	SNR
16 Cyg A	HR 7503	HI.20060903.23090	3721-7971	147
16 Cyg B	HR 7504	HI.20070826.40719	3721-7969	112
HD 109749 A	HD 109749	HI.20110412.33419	3721-7969	102
HD 109749 B	CD-40 7393B	HI.20050627.24308	3800-6423	90
HD 195019 A	HO 131A	HI.20050625.43149	3683-4862, 6545-7970	143
HD 195019 B	HO 131B	HI.20051219.18704	3682-4875, 6544-7969	117
83 Leo A	LHS 2407	HI.20060112.51171	3723-7971	151
83 Leo B	LHS 2408	HI.20060112.51421	3801-7971	162

of 3 distinct lines at 7771, 7774, and 7775Å, and is known to suffer from non-LTE effects (Ramírez *et al.*, 2009), which are not accounted for in my analysis. The non-LTE effects may cause the oxygen abundances reported in this study to be slightly underestimated in some cases.

2.1.4 Measurement of Equivalent Widths

The Equivalent Width (EW) of an absorption line is a single quantity used to describe the overall strength of an absorption line. Equivalent widths can be measured manually (requiring direct inspection of each spectral line), and there are many routines available to automate this measurement process. The equivalent width is the necessary width of a perfectly absorbing feature such that the total removed energy is the same (Arnett, 1996). The equivalent width of an absorption line (in which I_ν is the line intensity, and I_C is the corresponding continuum intensity) is written in terms of frequency as:

$$EW_\nu = \int_{line} \left(1 - \frac{I_\nu}{I_C}\right) d\nu$$

Manual: IRAF splot

The IRAF *splot* function allows a user to view a spectrum and interactively fit individual line profiles, selecting appropriate continuum points, selecting the type of line profile, and even deblending multiple spectral features. The resulting fitted line profile gives the line's measured equivalent width. In this work, *splot* was used to determine the line centers of well known lines in measuring each spectrum's RV offset. Manual *splot* EW measurements were also used to ensure that the automated system (ARES) was producing consistent results. Using *splot* for these measurements is a much more time-consuming process, but it is also less prone to measurement errors (such as an automated program selecting the wrong line to measure), as the user can visually inspect the spectrum to ensure the correct line is being measured. The downside to an interactive measurement approach (other than the time required) is that the results obtained by various users, based on differences in technique, can differ in EW by up to 10 mÅ for larger lines.

Automated: ARES

To quickly measure the Equivalent Widths for the entire linelist, the Automatic Routine for line Equivalent widths in stellar Spectra (ARES) was used (Sousa *et al.* (2007)). ARES has a multi-step process to analyze a given spectrum line by line, using an input linelist. First, ARES calculates a local continuum around the line, then fits gaussians to all nearby lines, finally yielding the exact position, EW, FWHM, and other information for the line of interest. By using a script to run ARES on each order, a linelist consisting of several hundred lines can be measured (across many orders) in a short period of time.

To run, ARES requires a set of input parameters (contained in the file *mine.opt*). In units of pixels, *smoothder* defines the size of a filter used to smooth the derivatives of the spectrum, which are used to identify line centers. The continuum is fit within a region around each line, the size of which is given in Å by *space*. The minimum spacing (in Å) between consecutive lines is limited by *lineresol*. The smallest acceptable EW (in mÅ) is given by *miniline* - smaller results will be ignored. Finally, *rejt* is used by *ARES* to determine which points to use in fitting the continuum - spectra with lower SNR should also use a lower *rejt* to ensure correct placement of the continuum. Typical values for each parameter as used in this analysis are given in Table 2.3.

Table 2.3: Typical ARES parameter values

Parameter name	Value
smoothder	3
space	5.0
rejt	0.985
lineresol	0.1
miniline	2

Ares validation

To validate ARES for use, a comparison of Equivalent Widths was made between the ARES measurements and the manual SPLOT measurements. For two data sets (16 Cyg A and HD 195019 A), all lines were measured with both SPLOT and ARES methods. Comparison of these measurements are given as Figures 2.3 and 2.4. The results show that ARES does not preferentially over- or under-measure equivalent widths, but there is some scatter around the expected 1:1 trend. There are also some

outlying points, indicating lines that may have been mis-identified or mis-measured by ARES. This could be due to ARES choosing the wrong line center and measuring the wrong line entirely, or from not properly deblending lines. Attempting to deblend a single line would result in ARES underestimating the EW, while treating a blended line as a single line would result in an overestimation of the EW. Major outlying lines are labeled with their element and ionization state.

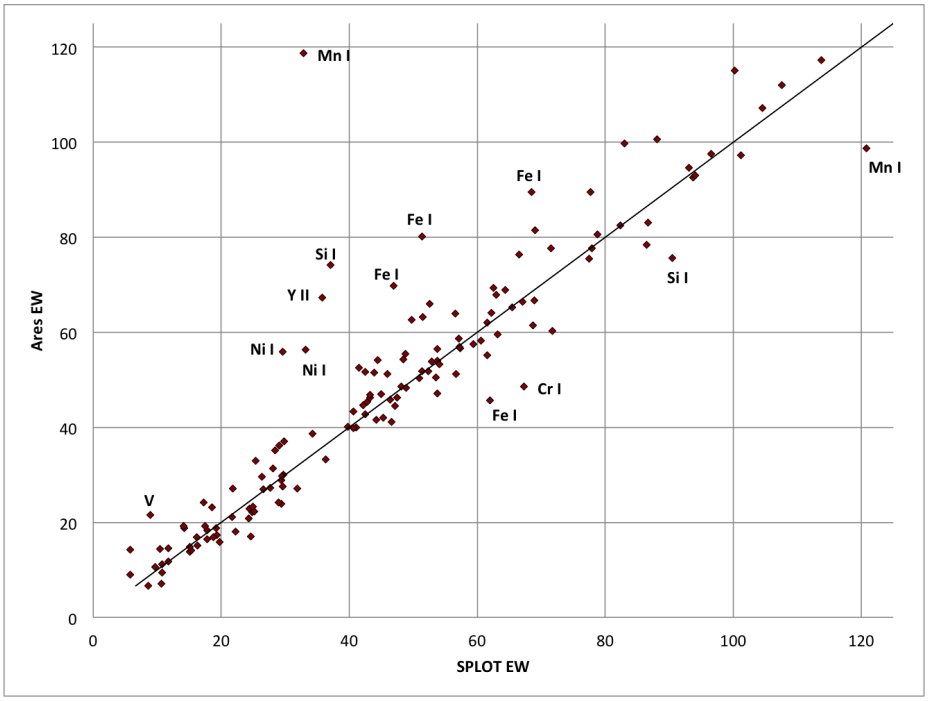

Figure 2.3: Comparison of EW measurements made with IDL splot against ARES for 16 Cyg A

In the case of 16 Cyg A, the outlying line measurements corresponded to the following elements: Fe (4 lines), Ni (2 lines), Mn (2 lines), Si (2 lines), Cr, Y and V (1 line each). For elements with few overall lines (V, Mn, Y and Cr in particular), these anomalous lines have a significant impact on both the line uncertainty σ_μ and the overall abundance.

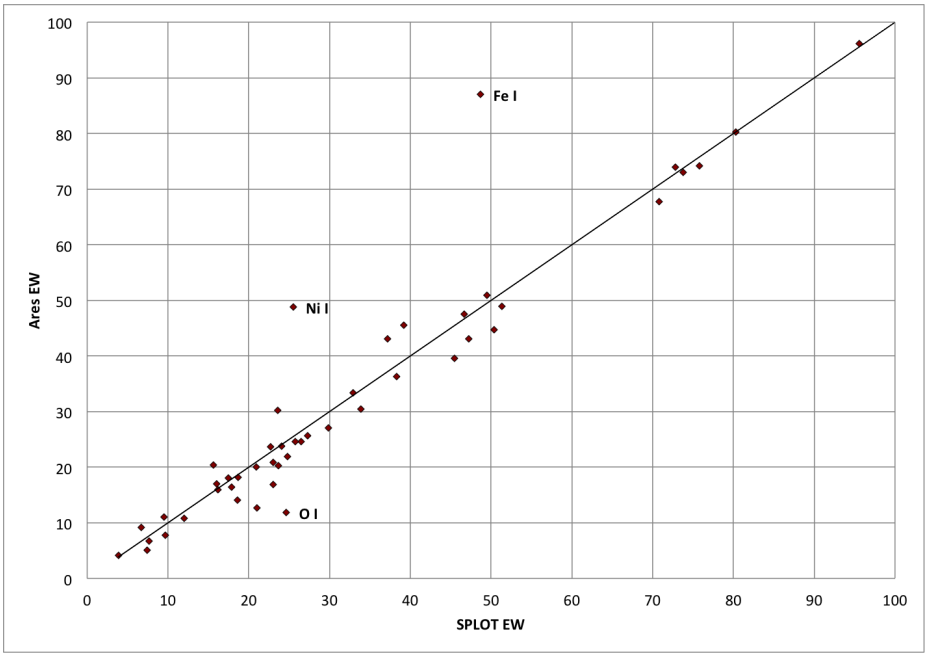

Figure 2.4: Comparison of EW measurements made with IDL splot against ARES for HD 195019 A (fewer lines could be measured in this data set due to gaps in the spectral coverage)

2.1.5 Abundance Analysis

The spectral synthesis program MOOG (Sneden (1973)) was used for abundance analysis. MOOG calculates absorption from elemental and molecular species in a stellar atmosphere, assuming local thermodynamic equilibrium (LTE). MOOG has several driver functions for different modes of operation; in this work the *abfind* driver is used. MOOG's *abfind* driver uses a curve-of-growth analysis to derive an elemental abundance corresponding to input data given for each spectral line.

MOOG requires a stellar atmosphere model as input; for this work the updated *ATLAS 9* 1-d parallel plane stellar atmosphere models were used (based on work of Kurucz (1993)). ATLAS 9 models the stellar atmosphere as a series of 72 layers, each with its own temperature and pressure, with the assumption of LTE held within each layer. Radiative processes, including line absorption, are then solved by MOOG through each of these layers as photons escape through the stellar atmosphere.

Several stellar parameters must be set for each atmosphere model: Effective temperature T_{eff}, Surface Gravity $Log(g)$, Metallicity $[Fe/H]$, and Microturbulent Velocity (ξ). Determining these parameters for each star is an important step in the abundance analysis. One well-known method, known as an Ionization/Excitation balance, uses many line measurements of a single element, in multiple ionization states, to determine these stellar parameters directly from the same data used for abundance analysis. Iron is the typical element choice, due to the vast number of Fe I and Fe II lines occurring in the visible spectrum.

The ionization/excitation balance is an iterative process based on altering the stellar atmosphere parameters until each measured iron line derives a similar abundance. Specifically, there should be no correlation between derived Fe abundance and any spectral line property (ionization state, excitation potential, or reduced equivalent width). Minimizing these correlations indicates that the chosen atmosphere model is self-consistent with the observed spectrum (Bubar and King, 2010).

The absorption due to a specific transition at a given temperature is connected to the excitation potential (EP) of the transition; therefore any trend between EP and derived abundance indicates an inaccurate temperature. The microturbulent velocity represents differing velocities of gas parcels on a star's surface. This velocity difference contributes to a widening of spectral features, and is therefore related to line's reduced equivalent width ($rEW = log(EW/\lambda)$). Therefore, a self-consistent microturbulent velocity will result in no correlation between derived abundance and rEW. Finally, lines of different ionization states will have different pressure sensitivities, allowing stellar surface gravity to be determined by matching overall derived abundances of iron between both ionization states.

To determine appropriate stellar parameters, MOOG was used to calculate abundances and correlations for all measured Fe I and Fe II lines in a spectrum. As a first

estimation, stellar parameters from other literature studies (or from a star's spectral type) were used. The stellar parameters of the atmosphere model (T_{eff}, $Log(g)$, $[Fe/H]$, and (ξ)) were then gradually altered, in order to reduce correlations as much as possible. As this was done, the linelist was periodically checked and edited to remove outlying Fe lines, which could impede the convergence process. Any Fe line yielding an abundance differing from the average by greater than 0.5 in $Log(N)$ was removed from the analysis. This typically corresponded to 1 to 1.5 σ_L (standard deviations of derived abundances from all Fe lines).

2.1.6 Stellar Parameters from literature

For comparison and validation, stellar parameters reported in the literature were also obtained for our stellar sample (as given in Table 2.4). When possible, sources that derived parameters using a similar method (Iron ionization/excitation balance) were used.

Table 2.4: Stellar parameters for target stars as reported by other studies

Star	Temperature	Log(g)	ξ	[Fe/H]	Source
16 Cyg A	5780	4.35	0.85	0.09	Heiter and Luck (2003)
16 Cyg B	5800	4.4	0.95	0.06	Heiter and Luck (2003)
HD 109749 A	5899	4.31	1.13	0.32	Sousa *et al.* (2006)
HD 109749 B	-	-	-	-	(no published parameters)
HD 195019 A	5830	4.3	1.05	0.05	Heiter and Luck (2003)
HD 195019 B	-	4.63	-	-	Takeda *et al.* (2007)
83 Leo A	5650	4.45	1	0.40	Heiter and Luck (2003)
83 Leo B	5250	4.60	1.2	0.36	Heiter and Luck (2003)

2.1.7 Uncertainty Analysis

The derived abundances are affected by three sources of uncertainty: uncertainty in the measured EW of individual lines, uncertainty in the derived stellar parameters ($\sigma_T, \sigma_{SG}, \sigma_\xi$), and a spread of the abundances derived from several lines for a given element (σ_μ). Uncertainty in the measured EW from each individual line is not significant compared to the other two sources, and is not addressed here. The errors from each source arise independently, so the full uncertainty is given by the components added in quadrature:

$$\sigma_{Total} = \sqrt{\sigma_T^2 + \sigma_{SG}^2 + \sigma_\xi^2 + \sigma_\mu^2}$$

The derived abundance values are sensitive to the choices of adopted stellar parameters, so uncertainties in these inputs will carry through to the abundance results. The uncertainty in values chosen for each stellar parameter will contribute a term to the overall uncertainty in derived abundance. The abundance uncertainties depend on the specific lines used, as well as the given EW measurements for each line, and therefore must be calculated for each element in each star separately. All elemental abundances were re-derived (with the same input linelist) using high and low values for each parameter, while keeping the other parameters set to the nominal value. The parameter deviations used were: $\pm 150K$ in T_{eff}, ± 0.25 in $Log(g)$, and $\pm 0.30 km/s$ in ξ. These values are a good representation of the uncertainty encountered in this study in deriving stellar parameters using the Fe excitation balance method, and are also the same values used as parameter uncertainties in similar works (Schuler *et al.*, 2011b).

Half of difference in derived Log(N) for a given element between upper and lower stellar parameter inputs is taken as the uncertainty due to that parameter. For example, the uncertainty in Magnesium abundance due to temperature ($[Mg/H]\sigma_T$) is calculated as follows:

$$[Mg/H]\sigma_T = \frac{[Mg/H]_{T=T_0+150} - [Mg/H]_{T=T_0-150}}{2}$$

In this case, T_0 is the accepted temperature value. This process gives an uncertainty for each derived elemental abundance, and is repeated in the same fashion to generate uncertainty values for each parameter.

When using the *abfind* driver, MOOG derives an elemental abundance from each individual spectral line. For elements with more than one measured line, the overall elemental abundance is the averaged abundance from all lines. The standard deviation of line-derived abundances (σ_L) contributes to the intrinsic uncertainty present for multi-line elements (with N measured lines):

$$\sigma_\mu = \frac{\sigma_L}{\sqrt{N}}$$

The σ_μ uncertainty can be reduced by including many (reliably-measured) lines in the analysis.

Due to properties of the specific absorption lines, derived abundances of some elements are more sensitive to variations in each stellar parameter than others. Given the deviations used in this error analysis, the largest contribution to parameter uncertainty for most elements comes from σ_T. The elements with the highest temperature sensitivities are O, Ti I, V, Mn, Sr, and Mo. Elements derived using absorption features of partially ionized atoms have higher sensitivities to changes in Log(g), particularly Ti II, Nd II, Eu II, Ce II, and Sc II. Changes in microturbulent velocity

most strongly affected the abundances of Sr, Y II, and Ba II. Some elements, Si in particular, were found to be relatively insensitive to changes in all stellar parameters.

2.1.8 Abundance conventions

Elemental Abundance values represent the relative number density of atoms of a given element found in a star's photosphere. There are two conventions used to quantify this abundance: $Log(N)$ and $[m/H]$. $Log(N)$ is simply the (base-10) logarithm of the number density of atoms, normalized to the defining value of Hydrogen as $Log(N_H) \equiv 12$. These values are often compared to solar abundances, denoted by the bracket notation $[Fe/H]$ (using iron here as the example). In this work, the internal MOOG solar values are used for comparison, which come from Anders and Grevesse (1989).

$$[Fe/H] = Log_{10}\left(\frac{N_{Fe}}{N_H}\right)_{\star} - Log_{10}\left(\frac{N_{Fe}}{N_H}\right)_{\odot}$$

2.2 Derived Abundances for each system

Shown in the tables below are the adopted stellar parameters and resulting compositions (with uncertainties) for each stellar system. Abundances [m/H] are given relative to solar values. Identical linelists were used between stars in a given system, but not necessarily between all systems (due to differences in spectral coverage).

2.2.1 16 Cyg

Table 2.5: Abundances for 16 Cyg

	16 Cyg A		**16 Cyg B**	
Temp	**5898**		**5883**	
Log(g)	**4.76**		**4.77**	
$[Fe/H]$	**0.06**		**0.116**	
microturb.	**2.74**		**2.12**	
Element	**[m/H]**	**error**	**[m/H]**	**error**
C	-0.05	0.15	-0.08	0.12
O	-0.12	0.15	-0.11	0.13
Na	-0.06	0.10	0.01	0.10
Mg	0.18	0.08	0.05	0.11
Al	0.11	0.08	0.17	0.08
Si	-0.06	0.11	0.08	0.06
S	0.31	0.17	0.28	0.23
K	-0.20	0.16	0.10	0.17
Ca	-0.07	0.15	0.05	0.14
Sc II	0.26	0.11	0.24	0.14

Ti I	0.10	0.17	0.15	0.17
Ti II	0.19	0.10	0.25	0.10
V	-0.01	0.20	0.22	0.25
Cr	0.01	0.19	0.23	0.18
Mn	0.22	0.23	0.47	0.28
Fe I	0.05	0.09	0.12	0.10
Fe II	0.04	0.13	0.16	0.15
Ni	0.02	0.10	0.12	0.10
Cu	-0.06	0.16	-0.05	0.14
Zn	-0.19	0.21	-0.32	0.08
Y II	-0.03	0.12	-0.01	0.29
Ba II	-0.13	0.30	0.06	0.24
Ce II	0.12	0.12	0.18	0.13
Nd II	0.49	0.11	0.53	0.11
Eu II	0.31	0.11	0.41	0.10

16 Cyg, being a long-known bright, binary, planet-hosting system, has been the target of multiple detailed composition studies including both A and B components:Gonzalez (1998) (15 elements), Schuler *et al.* (2011a) (15 elements), and Ramírez *et al.* (2011) (24 elements). In this analysis, 28 elements were measured for 16 Cyg A, and 29 for 16 Cyg B. The oxygen abundance in 16 Cyg B was calculated using both the 6363Å line and the infrared triplet; in the A component the 6363Å line could not be measured due to a gap in spectral coverage.

Stellar parameters for 16 Cyg A and B have been previously reported by Schuler *et al.* (2011a) ($T_{eff} = 5796, 5753$, $Log(g) = 4.38, 4.40$, $[Fe/H] = 0.07, 0.05$, $\xi = 1.45, 1.35$) and Heiter and Luck (2003) ($T_{eff} = 5780, 5800$, $Log(g) = 4.35, 4.4$, $[Fe/H] =$

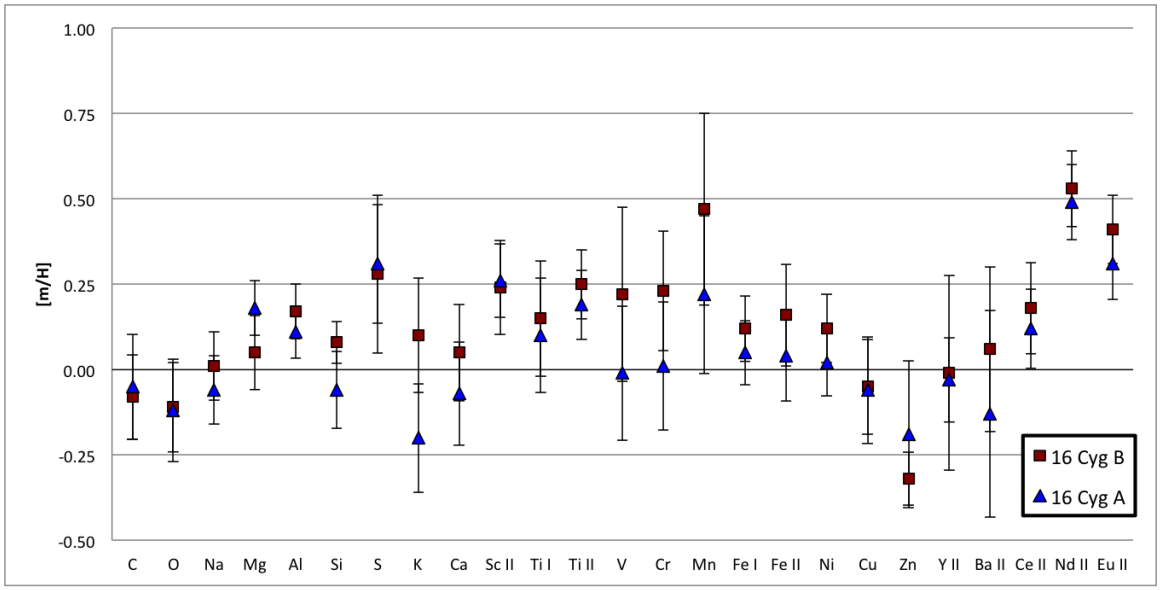

Figure 2.5: Elemental abundances of 16 Cyg A and B (Host)

$0.09, 0.06, \xi = 0.85, 0.95$). Compared to the parameters used by Schuler *et al.* (2011a), I find each component of 16 Cyg to be slightly hotter, with effective temperatures higher by 100-130 K. This small difference falls within my estimated uncertainty. However, the Log(g) values (above 4.7) and ξ values (above 2.2) are significantly higher than used in other studies. In the case of the surface gravity, these values were used because they resulted in the best balance the Fe I and Fe II abundances, however these values are unphysically high.

I find the 16 Cyg system to be sub-solar in Carbon and Oxygen in this analysis, a result which is not consistent with other studies. Zn is also found to be notably sub-solar. Most elements are found to match well with other studies, with differences typically less than .10 dex, meaning that my results fall within reported errors in both studies for most elements. Nd and Eu are found to be notably enhanced in both components, above .3 dex from solar values. In general, these results are consistent with the 16 Cyg system having two very chemically similar components, with compositions very similar to our sun.

2.2.2 83 Leo

Table 2.6: Abundances for 83 Leo

	83 Leo A		**83 Leo B**	
Temp	**5700**		**5700**	
Log(g)	**4.5**		**4.55**	
$[Fe/H]$	**0.35**		**0.32**	
microturb.	**1.4**		**1.0**	
Element	**A dex**	**error**	B dex	Error
C	-0.04	0.20	-0.20	0.16
O	-0.12	0.18	-0.71	0.25
Na	0.37	0.13	1.19	0.38
Mg	0.42	0.18	0.73	0.16
Al	0.47	0.09	0.85	0.10
Si	0.32	0.13	0.16	0.08
S	0.58	0.48	-0.01	0.63
K	0.45	0.18	0.95	0.19
Ca	0.52	0.22	0.93	0.22
Sc II	0.51	0.14	0.72	0.34
Ti I	0.49	0.19	1.22	0.21
Ti II	0.17	0.11		
V	0.69	0.20	1.66	0.27
Cr	0.43	0.19	0.99	0.23
Cr II	1.19	0.35	1.25	0.45
Mn	1.46	0.33	1.58	0.29

Fe I	0.34	0.12	-0.05	0.10
Fe II	0.14	0.15	0.14	0.13
Co	0.02	0.07	0.39	0.37
Ni	0.50	0.12	0.57	0.13
Cu	0.64	0.25	0.91	0.27
Zn	0.21	0.21	0.24	0.19
Sr	0.14	0.23	1.09	0.23
Y II	0.36	0.29	0.23	0.28
Zr II	0.21	0.11	0.00	0.11
Mo	0.09	0.15	1.16	0.21
Ba II	0.49	0.25	0.74	0.19
Ce II	0.41	0.12	0.63	0.20
Nd II	0.52	0.12	0.83	0.18
Eu II	0.17	0.11	0.22	0.11

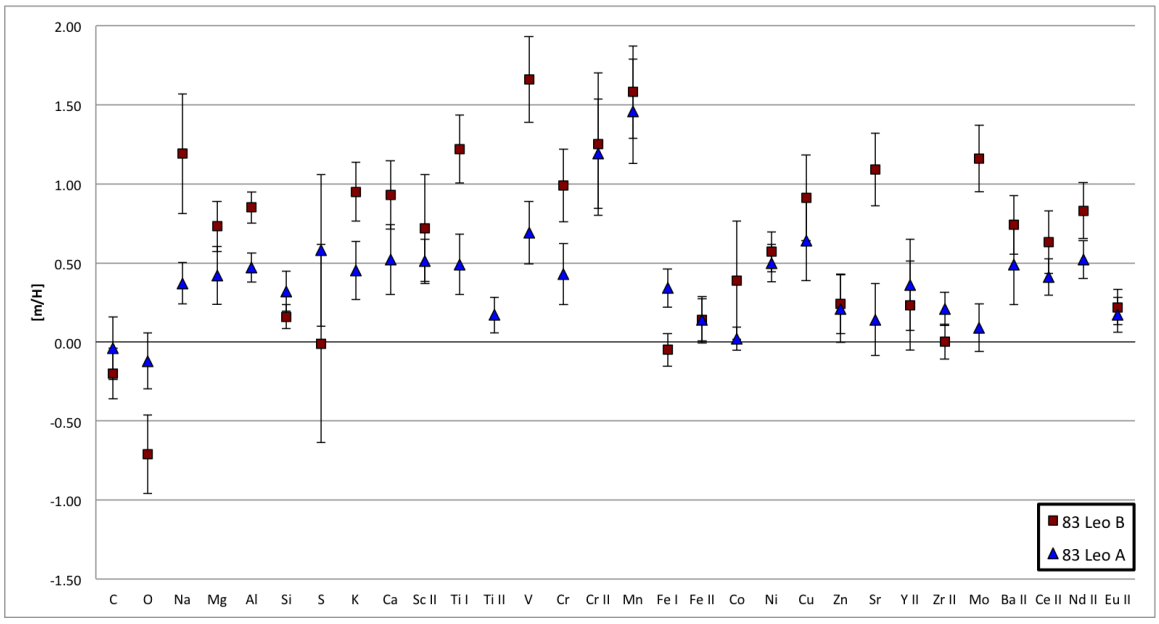

Figure 2.6: Elemental abundances of 83 Leo A and B (Host)

Surprisingly, despite being a long-known planet hosting binary system, 83 Leo has not been the target of any detailed differential composition studies including both components. 83 Leo A (HD 99491) itself has had several detailed composition studies, namely Feltzing and Gonzalez (2001) (12 elements), and Takeda (2007)(15 elements). 83 Leo B (HD 99492), with at least 2 known planets, has been analyzed only in terms of single-element studies, including Iron (Heiter and Luck, 2003), Oxygen (Ecuvillon *et al.*, 2006b), Beryllium (Gálvez-Ortiz *et al.*, 2011), and Lithium (Favata *et al.*, 1996).

The study by Heiter and Luck (2003) reported the stellar parameters for 83 Leo A and B as: $T_{eff} = 5620, 5250$, $Log(g) = 4.45, 4.60$, $[Fe/H] = 0.40, 0.36$, $\xi = 1.0, 1.2$. In this study, the excitation balance produced best-fit temperatures of 5700 K for both components of 83 Leo, which is hotter than is found in other studies (and much hotter than the stars' spectral types). 83 Leo B is found to have a higher surface gravity, consistent with its type as a main sequence star (versus the subgiant A component), although Heiter and Luck (2003) finds a larger difference in surface gravity between the two components. Contrary to Heiter and Luck (2003), I find Leo A to have the higher microturbulent velocity of the pair.

Consistent with their known status as super-metal rich stars, I find both A and B components in 83 Leo to be enriched (compared to the sun) in every element measured, with the exception of Oxygen. Abundances of Ca, Cr, Mn, and Ni for 83 Leo A are found to be significantly higher than those reported by Feltzing and Gonzalez (2001) or Takeda (2007), although Co is found to be lower. Similar to the A component, derived abundances in the B component for Cr and Mn are very high. Na, V, and Ti are also found to have a very high abundance in 83 Leo B.

Both components in 83 Leo were found to have a sub-solar oxygen abundance, with the B component being especially depleted. The oxygen abundance for 83 Leo A was derived using the infrared triplet and the 6155 Å line. Individual line results were

inspected for 83 Leo B, and the contribution from the 7771 Å line (known to be the most effected by non-LTE effects) was found to be much lower than the other triplet lines, and was rejected from the average. Even after this rejection, the remaining O lines (6363, 7774, and 7775 Å) yield an [O/H] value of -0.71 ± 0.25. This is over 0.7 dex lower than the more thorough, NLTE treatment by Ecuvillon *et al.* (2006b) ($[O/H] = 0.01 \pm 0.08$).

2.2.3 HD 109749

Table 2.7: Abundances for HD 109749

	HD 109749 A		**HD 109749 B**	
Temp	5899		5175	
Log(g)	4.31		4.1	
$[Fe/H]$	0.32		0.1	
microturb.	1.13		1.1	
Element	**A dex**	**error**	**B dex**	**Error**
C	0.09	0.14	0.39	0.21
N	-0.03	0.14		
O	0.09	0.16	0.54	0.56
Na	0.4	0.10	-0.11	0.12
Mg	0.14	0.21	0.05	0.13
Al	0.3	0.08		
Si	0.41	0.11	0.3	0.07
S	0.5	0.32		
K	0.51	0.17		
Ca	0.27	0.15	-0.37	0.21

Sc II	0.61	0.22	0.57	0.39
Ti I	0.29	0.17	-0.46	0.21
Ti II	0.14	0.11		
V	0.35	0.17	-0.48	0.31
Cr	0.57	0.17	0.1	0.21
Cr II	1.07	0.47	1.51	0.42
Mn	1.18	0.27	0.05	0.34
Fe I	0.32	0.14	-0.09	0.10
Fe II	0.32	0.21	0.48	0.18
Co	0.66	0.41	0.22	0.49
Ni	0.46	0.13	0.21	0.11
Cu	1.05	0.36	0.23	0.23
Zn	0.34	0.09	0.38	0.20
Sr	-0.04	0.19	-0.89	0.22
Y II	0.76	0.27	0.74	0.38
Zr II	0.35	0.11	0.92	0.15
Mo	0.2	0.15	-0.5	0.17
Ba II	0.54	0.19	0.24	0.20
Ce II	0.11	0.15	-0.1	0.12
Nd II	1.21	0.18	0.32	0.37
Eu II	0.08	0.11		

The planet-hosting HD 109749A has been the target of spectroscopic studies by Sousa *et al.* (2006) for stellar parameters and [Fe/H] = +0.32), and Petigura and Marcy (2011) for the C/O ratio. In addition to carbon ([C/H] = +0.28) and oxygen ([O/H] = -0.02) abundances, Petigura and Marcy (2011) also report values for nickel

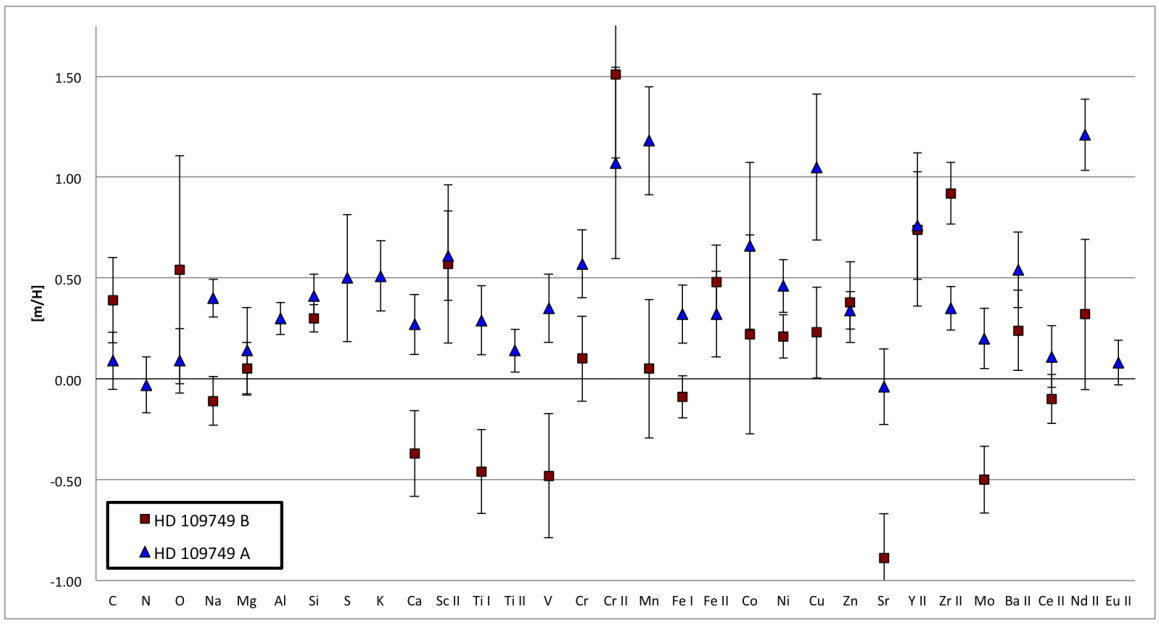

Figure 2.7: Elemental abundances of HD 109749 A (Host) and B

abundance ([Ni/H] = +0.38), which are a by-product of their O abundance calculations. No published literature references could be found regarding abundances of the B component. Oxygen abundance was derived using the 6155, 7771, 7774, and 7775 Å lines for HD 109749 A, and the 6155 and 6363 Å lines for HD 109749 B (in both cases due to available spectral coverage).

Previously published stellar parameters for HD 109749A from Sousa *et al.* (2006) (T_{eff} = 5899, $Log(g)$ = 4.31, $[Fe/H]$ = 0.32, ξ = 1.13) were found to satisfy the excitation/ionization balance, and were adopted for this study. The B component was found to have a higher temperature (5175), and lower surface gravity ($Log(g)$ = 4.10) than expected for a main-sequence K5V star.

In this work, HD 109749A is found to have lower carbon and higher oxygen values than previously reported: [C/H] = +0.09 and [O/H] = +0.09. The A component is found to be super-solar in most elements, particularly for the cases of Cr, Mn, and Cu. The B component is found to be significantly depleted relative to solar in Ca, Ti, V, Sr, and Mo, but to have an Fe abundance near solar.

2.2.4 HD 195019

None of the available datasets for HD 195019 on KOA included full spectral coverage with all three HIRES CCDs. The data used here covered only CCDs 1 and 3, corresponding to 3682 - 4875 Å, and 6544 - 7970 Å, with a gap between. For this reason, fewer lines could be measured, allowing for a total of 50 measured lines. Due to the smaller number of lines, it was feasible to use SPLOT to measure each line manually.

Table 2.8: Abundances for HD 195019

	HO 131 A		**HO 131 B**	
Temp	6000		5585	
Log(g)	4.75		4.7	
[Fe/H]	0.05		0	
microturb.	2.4		3.05	
Element	**A dex**	**error**	**B dex**	**Error**
C	-0.02	0.14	0.27	0.18
N	0.24	0.14	0.60	0.17
O	-0.19	0.15	0.21	0.19
Mg	0.15	0.08	-0.17	0.08
Al	0.14	0.08	-0.02	0.10
Si	-0.17	0.02	-0.26	0.04
S	0.14	0.11	0.44	0.14
K	0.04	0.16	-0.17	0.17
Ca	0.11	0.16	-0.31	0.17
Sc II	0.32	0.11	0.25	0.11

Ti I	0.16	0.14	-0.99	0.15
Ti II	0.14	0.11	0.14	0.11
Fe I	0.14	0.10	-0.09	0.08
Fe II	-0.19	0.11	0.31	0.15
Ni	-0.08	0.14	-0.34	0.16
Zn	-0.36	0.08	-0.45	0.08
Sr	-0.39	0.14	-0.78	0.16
Y II	-0.46	0.11	-0.58	0.11
Ce II	0.19	0.11	0.17	0.14
Eu II	0.05	0.11	0.55	0.11

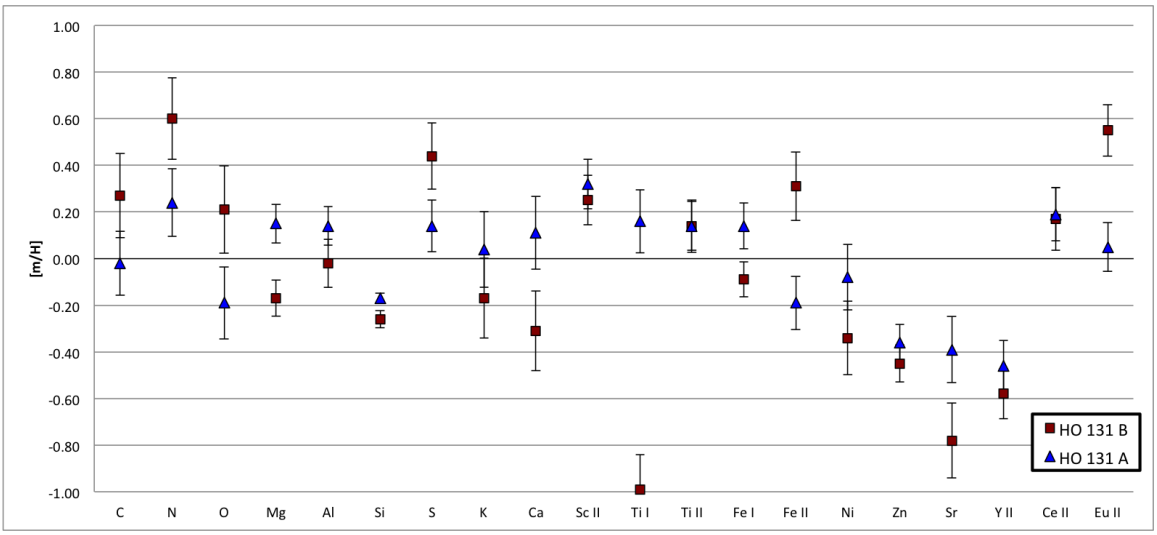

Figure 2.8: Elemental abundances of HD 195019 A (Host) and B

Several studies have investigated the chemical composition of planet-host HD 195019 A, however there have been no detailed studies of the B component composition beyond Log(g). Component A has been studied by Delgado Mena *et al.* (2010) (6 elements important for terrestrial mineralogy), Petigura and Marcy (2011) (Fe, C, O, and Ni), Schuler *et al.* (2011b) (15 elements), and Brugamyer *et al.* (2011)

(Si, O, and Fe). Oxygen abundance was derived for both components using only the infrared triplet.

Heiter and Luck (2003) report the stellar parameters of HD 195019 A to be (T_{eff} = 5830, $Log(g)$ = 4.3, $[Fe/H]$ = 0.05, ξ = 1.05). I find the surface gravity to be significantly higher ($Log(g)$ = 4.75), and the temperature (6000 K) and microturbulence (2.40) to be slightly higher. Takeda (2007) report the surface gravity of HD 195019 B to be 4.63. I find the B component to have slightly higher surface gravity, and a very high temperature and microturbulent velocity (considering its spectral type K3V).

Compared to other systems in this sample, the chemical abundances derived from HD195019 fall within smaller uncertainty values. This may be due in part to the virtue of measuring each line by hand in splot, reducing the number of mis-measured or incorrectly identified lines. For HD 195019 A, we find N, S, and Sc, to be more plentiful than reported by Schuler *et al.* (2011b), yet also find Si and Zn to be less abundant. Both components are found to have overall [Fe/H] near solar.

2.2.5 Effect of Stellar Parameter selection

As compared to other studies in the literature, this work differs in the linelist, the individual line measurements, and the adopted stellar parameters. Each of these factors contributes to the difference of derived abundances between this and other studies. To compare these factors, the effect of stellar parameter choice was investigated in particular. In other words, how much of the differences between studies can be attributed to the differences in adopted stellar parameters? To address this, the abundances of several stars were re-calculated, assuming the same stellar parameters used by other studies (Schuler *et al.* (2011a), Schuler *et al.* (2011b)) instead of the stellar parameters resulting from the ionization/excitation balance. For these calcu-

lations, the input data (including linelists and measured EWs) were the same as used for the abundance calculations elsewhere in this work. These re-derived abundances (with literature stellar parameters), the abundances from the corresponding studies, as well as abundances from this work, are shown in Figures 2.9 and 2.10.

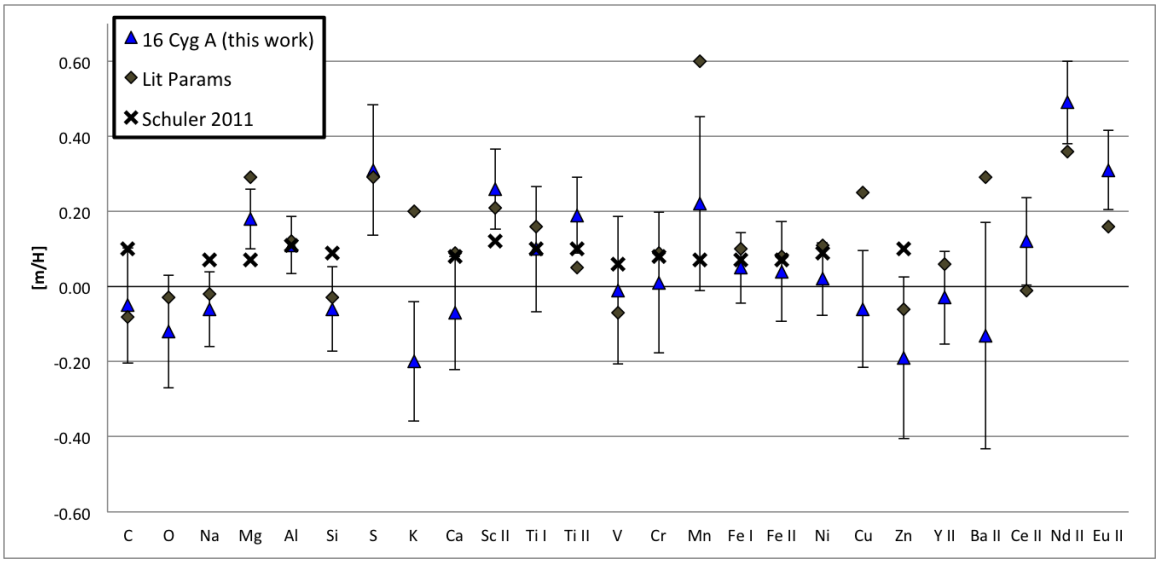

Figure 2.9: Elemental Abundances in 16 Cyg A, using stellar parameters from this work ($T_{eff} = 5898$, $Log(g) = 4.76$, $[Fe/H] = 0.06$, $\xi = 2.74$), as well as those from Schuler *et al.* (2011a) ($T_{eff} = 5796$, $Log(g) = 4.38$, $[Fe/H] = 0.07$, $\xi = 1.45$)

Adopting stellar parameters from Schuler *et al.* (2011a) yields derived abundances closer to the results of that study for about half of the 16 elements analyzed in both studies. The remaining elements show either negligible change or deviation away from the results of Schuler *et al.* (2011a). For some elements (K, Mg, Mn, Cu, Ba, Ce, Eu, Nd), the literature parameters yield abundances outside the error bars of this study. These results show that the selection of stellar parameters, while responsible for some of the discrepancies between this study and previous results, cannot account for differences in all elements.

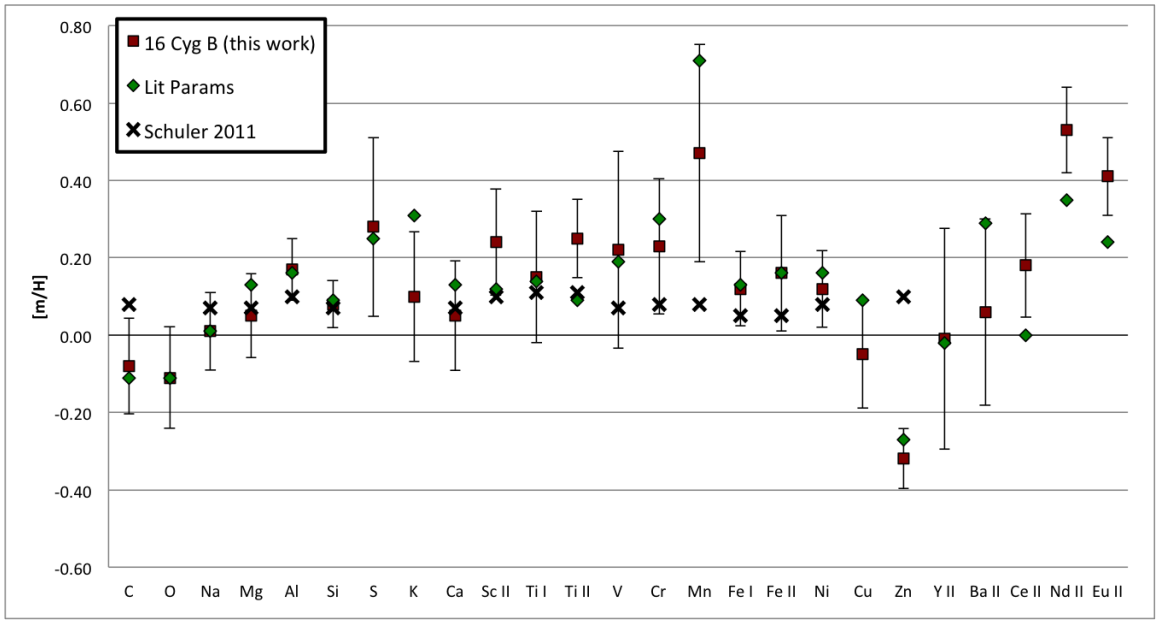

Figure 2.10: Elemental Abundances in 16 Cyg B, using stellar parameters from this work ($T_{eff} = 5883$, $Log(g) = 4.77$, $[Fe/H] = 0.116$, $\xi = 2.12$), and from Schuler *et al.* (2011a) ($T_{eff} = 5753$, $Log(g) = 4.40$, $[Fe/H] = 0.05$, $\xi = 1.35$)

2.2.6 Outlying Abundances

Some elements are found to have very high (or low) abundances across many stars in our sample. This may reflect consistent errors in the methodology (an example being the outliers in Figure 2.3, most of which are likely due to mis-measurements by ARES), rather than true anomalies in the chemical compositions. Sulfur is found to have high abundances in most of the studied stars, but frequently with high line uncertainties as well (σ_μ). This could indicate that a single line (out of the 3 or 4 typically measured) is contributing to an anomalously high abundance. In many of the stars, Chromium could be measured in multiple ionization states, with neutral (Cr I) and singly ionized (Cr II) states having measurable absorption lines. While these two ionization states should ideally derive the same elemental abundance, the derived Cr II abundances are discrepantly high in many of the target stars. In cases with multiple Cr II lines, (σ_μ) is typically very high.

Some of the rare-earth elements measured in this study (La, Nd, and Hf in particular) are seen in extreme abundance in several stars. In some cases, these elemental abundances are found to differ from solar values by over 1.0 dex, representing a significant enrichment. In most cases, these elemental abundances are derived from a single line measurement, meaning that a single mismeasured line could lead to an erroneous abundance derivation. Furthermore, in the case of elements with only one line measured, no σ_μ was included in the uncertainty estimates, resulting in generally lower uncertainties than multi-line elements.

Chapter 3

CONCLUSION

In this chapter, I interpret and discuss the chemical compositions previously derived: 8 stars (occurring as two components of 4 binary systems), have been analyzed for a suite of between 18 and 28 elements, depending on available spectral coverage. Each binary system in this study has one component with at least one known exoplanet. First, I discuss the differential composition of each binary system - how does each star compare to its binary companion, in terms of elemental abundances? Do any compositional patterns exist between hosts vs. non-hosts across multiple systems? Also, I address some properties of the planetary systems that can be connected to stellar composition, including preliminary measurements of system-wide C/O and Mg/Si ratios. Also, the implications of system composition are discussed in terms of possible planet formation, by analyzing trends of elemental abundance vs. elemental condensation temperature.

3.1 Differential Comparisons

One of the motivations of this work is to analyze the differential composition of these binary systems - that is, how do the stars within each multiple system vary chemically with respect to each other? Presumably, both stars formed out of the same nebular material, meaning their initial compositions should be nearly identical. Therefore, any significant observed differences in composition should be due to planet formation or other subsequent events (such as the re-accretion of planetary material).

Table 3.1 and Fig. 3.1 show the differential abundances for each system. Only elements with measurements in both stars could be compared. The values have all been calculated with respect to planet-hosting status as follows:

$$\Delta x = Log(N_x)_{Host} - Log(N_x)_{Non-host}$$

The uncertainty in differential abundance for a given element is simply the sum of uncertainties from the abundance of each star.

Table 3.1: Differential Abundances

	16 Cyg		**83 Leo**		**HD 109749**		**HD 195019**	
Element	**B-A**	**error**	**B-A**	**error**	**A-B**	**error**	**A-B**	**error**
C	-0.03	0.28	-0.16	0.36	-0.3	0.35	-0.29	0.32
N							-0.36	0.32
O	0.01	0.28	-0.59	0.43	-0.45	0.73	-0.4	0.34
Na	0.07	0.20	0.82	0.51	0.51	0.22		
Mg	-0.13	0.19	0.31	0.34	0.09	0.35	0.32	0.16
Al	0.06	0.16	0.38	0.19			0.16	0.19
Si	0.14	0.17	-0.16	0.20	0.11	0.18	0.09	0.06
S	-0.03	0.41	-0.59	1.11			-0.3	0.25
K	0.30	0.33	0.5	0.37			0.21	0.33
Ca	0.12	0.29	0.41	0.44	0.64	0.36	0.42	0.33
Sc II	-0.02	0.24	0.21	0.48	0.04	0.61	0.07	0.21
Ti I	0.05	0.34	0.73	0.40	0.75	0.38	1.15	0.29
Ti II	0.06	0.20					0	0.22
V	0.23	0.45	0.97	0.47	0.83	0.48		
Cr I	0.22	0.36	0.56	0.42	0.47	0.38		

Cr II			0.06	0.80	-0.44	0.89		
Mn	0.25	0.51	0.12	0.62	1.13	0.61		
Fe I	0.07	0.19	-0.39	0.22	0.41	0.25	0.23	0.17
Fe II	0.12	0.28	0	0.28	-0.16	0.40	-0.5	0.26
Co			0.37	0.45	0.44	0.91		
Ni	0.10	0.20	0.07	0.25	0.25	0.24	0.26	0.30
Cu	0.01	0.30	0.27	0.52	0.82	0.59		
Zn	-0.13	0.29	0.03	0.40	-0.04	0.29	0.09	0.16
Sr			0.95	0.46	0.85	0.41	0.39	0.30
Y II	0.02	0.41	-0.13	0.57	0.02	0.65	0.12	0.22
Zr II			-0.21	0.22	-0.57	0.26		
Mo			1.07	0.36	0.7	0.32		
Ba II	0.19	0.54	0.25	0.44	0.3	0.39		
La			-0.22	0.48				
Ce II	0.06	0.25	0.22	0.31	0.21	0.27	0.02	0.25
Nd II	0.04	0.22	0.31	0.30	0.89	0.55		
Eu II	0.10	0.21	0.05	0.22			-0.5	0.22

The overall chemical differences between binary components display a range of traits in the 4 systems studied here. 16 Cyg, in which both components have very similar spectral types (G3V and G1.5V), shows only minor chemical differences between the two components. The most disparate elements in 16 Cyg are K, V, Cr, and Mn, all having $0.2 < \Delta x \leq 0.3$, meaning that even these elements have overlapping error bars. This agrees with other studies (Schuler *et al.*, 2011a), which have shown the two components to be nearly chemically identical (with the exception of Li).

The chemical differences in the other systems are much more pronounced. 83

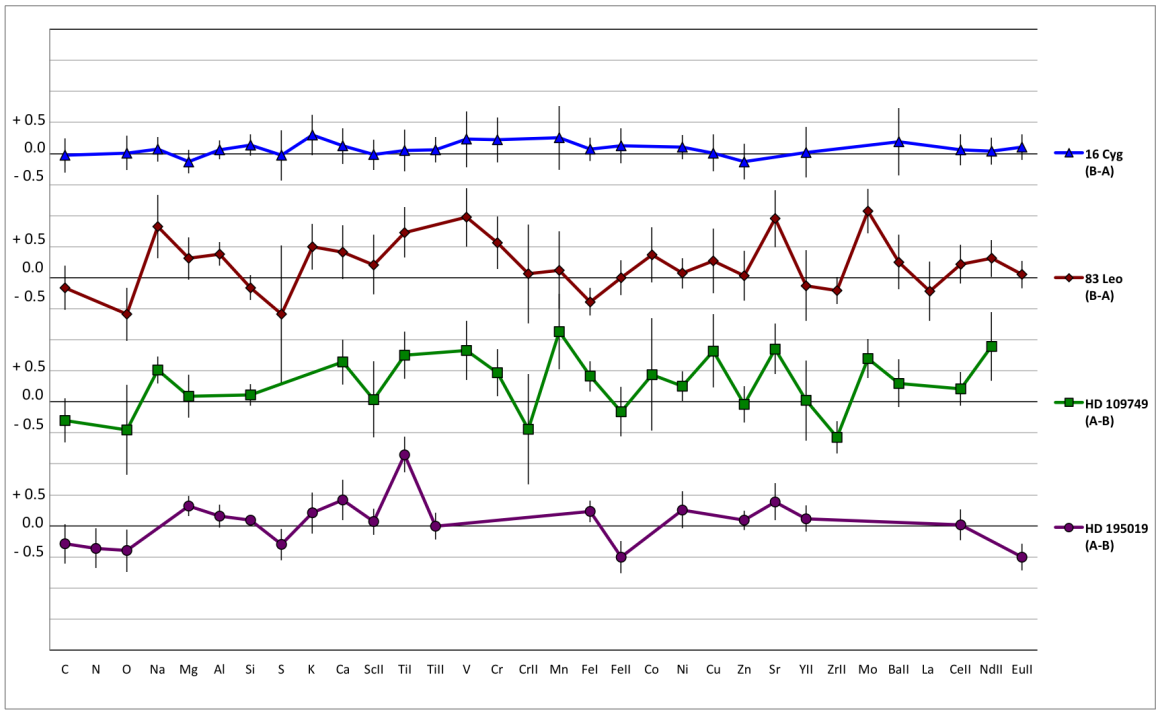

Figure 3.1: Differential compositions for each binary system

Leo B is deficient compared to its binary companion in O, but enriched (beyond uncertainty) in Na, Al, K, Ti, V, Sr, and Mo.

The HD 109749 shows the biggest overall difference between stars, with the planet-hosting A component is found to be statistically enriched relative to its companion in many elements: Na, Ca, Ti, V, Mn, Cu, Sr, Mo, and Nd. Zr is the only element found to be more abundant in HD 109749 B (beyond the abundance uncertainties).

The HD 195019 systems shows the A component to have a severe overabundance in Ti I, but this is likely a result of a very low Ti I measurement in the B component. Furthermore, the two stars are found to have quite similar Ti II abundances, arguing against any true difference in abundances. The Iron abundances also show discrepant patterns for ionization states, arguing against any real difference. N, O, and S are seen in higher proportions in the B component, while the A component has greater Mg, Ca and Sr.

Some elements show similar behavior between components across several binary systems. The elements C, N, O, S, and Zr are relatively depleted in most of the planet-host companions, although O, N, and Zr are the only elements in which this trend is beyond the combined elemental uncertainties. Elements found in notably greater abundance in the planet-hosting components (across multiple systems) include Na, Ca, V, and Mo. Strontium had the strongest result: in the 3 systems having measurable Sr lines, all planet hosts had Sr abundances far above ($\Delta[Sr] \gtrsim 0.4$) their non-host companions.

Several published studies seek to find correlations of individual element abundance to planet existence. Some studies, such as Beirão *et al.* (2005) and Gilli *et al.* (2006), find that planet hosts are also statistically enriched in other heavy elements (such as Al, Mg, Na, and others) in addition to Fe, but that these enrichments do not significantly deviate from what would be expected from galactic chemical evolution models for increasing metallicity.

Above what is accounted for by galactic chemical evolution, V and Mn were found in enriched abundances among planet-hosting stars by Bodaghee *et al.* (2003). Kang *et al.* (2011) also find Manganese abundance to be statistically higher in planet hosting stars, as compared to a non-host control sample. In the 3 binary pairs of this study that Mn was measured in, only HD109749 shows a notable Mn enrichment in the host star.

Silicon, as one of the most important rock-forming elements, has been studied with respect to planet occurrence by several groups. Robinson *et al.* (2006) report enrichment in Si and Ni for planet-hosting stars, both of which are explained by their core-accretion simulations. Brugamyer *et al.* (2011) look for trends in Si and O with respect to planet existence, and find a 99% probability that the planet detection rate depends on the Si abundance of a host star, even after after accounting for [Fe/H].

This is interpreted to mean that silicate grain nucleation is a critical step in the core-accretion process. In our 4 star systems, both host and non-host stars show silicon abundances very similar to their companions.

3.2 Trends with Condensation Temperature

The details of mineral condensation from a protoplanetary disc is a deep topic with many well-established references, including Lodders (2003), Ebel and Grossman (2000), and Ebel (2006). In summary, during the star formation process, a fraction of material is incorporated into a protoplanetary disc surrounding the star. The material in this disc is able to cool and gradually solidifies into solid mineral grains. Some elements (H and noble gasses) never solidify, existing as a gas and either being absorbed into a planetary or stellar atmosphere, or dissipating into the interstellar medium. Volatile elements are only able to condense in low-temperature environments, resulting in different types of ices. Refractory elements (including most metals) condense earlier from the protoplanetary disc, at high temperatures. The condensation temperature of an element, T_C, is the temperature below which an element in a gaseous state (in the protoplanetary disc) will condense into an initial mineral state.

The core-accretion model of planetary formation supports the observed planet-metallicity correlation by surmising that systems which are initially metal-rich will experience enhanced planet formation. In this case, the enhanced metallicity observed in planet-hosts is a primordial signature of the planet-forming environment.

Self-enrichment (as initially suggested by Gonzalez (1997)) provides an alternative, second-order effect which could also explain (or contribute to) this enhanced metallicity. In this scenario, a star could accrete volatile-depleted material from its protoplanetary disc, causing the photosphere to become enriched in high T_C elements. However, studies by Smith *et al.* (2001) and Ecuvillon *et al.* (2006a), despite finding

some stars with positive abundance trends in T_C, found no overall difference in T_C trends between planet-hosts and non planet-hosts.

Beyond a star simply having or lacking planets, the *type* of planetary system may have a detectable effect on self-enrichment trends. Meléndez *et al.* (2009) found the sun to be depleted in refractory ($T_C < 900K$) elements, as compared to 11 solar-twin stars. Ramírez *et al.* (2009) also found that most solar twins (85%) in a larger sample (64) were enhanced in more refractory elements as compared to the sun. One possible explanation for this is that the sun could not re-accrete as much refractory material from the protoplanetary disc, for it was locked up in the terrestrial planets. In this way, the "unusual" abundance pattern (deficiency of refractory elements) seen in the sun could be a sign of terrestrial planet existence. The "non-host" binary components in this study are not currently known to have any short-period giant planets, but smaller and more distant planets cannot be ruled out. Furthermore, true terrestrial planets would be beyond the current RV sensitivity for all components in this study, encouraging methods to infer such information indirectly.

Gonzalez *et al.* (2010) studied T_C trends in a wider range of stellar types (extending beyond solar-twins), and confirmed that stars with (giant) planets have more negative T_C trends than a sample without known planets. This negative trend was also found to be more pronounced in higher metallicity ($[Fe/H] > 0.1$) stars with planets. Ramírez *et al.* (2010) also confirm that a negative trend of abundance vs. T_C for refractory elements is a likely signature of terrestrial planets, using abundance results from six separate studies.

Schuler *et al.* (2011b) derived higher-precision abundances for a sample of stars with known giant planets and positive overall trends in [m/H] vs T_C, therefore being likely candidates for self-enrichment. While they confirm the overall positive [m/H] vs T_C trends in all stars, when only accounting for refractory elements, both positive

and negative trends in [m/H] vs T_C are observed. All stars with positive trends within refractory elements also possessed hot jupiters, supporting the idea that any terrestrial planets were previously accreted during inward Type 1 planetary migration (Ida and Lin, 2008). Stars with negative slopes were found to have planets with wider orbits, consistent with the idea that less planetary migration resulted in less self-enrichment of refractory elements.

In a similar fashion to previous studies, I compare the derived abundances in each system to the condensation temperatures of those elements. The condensation temperatures used (seen here as Table 3.2) are taken from the 50% condensation temperatures in a solar-system composition gas, as given by Table 8 of Lodders (2003) (these are the same values of T_C used by Schuler *et al.* (2011b) in their analysis). These values refer to a temperature at which 50% of an elemental species has condensed into solid condensate material, and 50% of the element is still in a vapor phase.

Table 3.2: Elemental condensation temperatures

Element	50% T_C
C	40
N	123
O	180
Na	958
Mg	1336
Al	1653
Si	1310
S	664
K	1006
Ca	1517

Sc	1659
Ti	1582
V	1429
Cr	1296
Mn	1158
Fe	1334
Co	1352
Ni	1353
Cu	1037
Zn	726
Sr	1464
Y	1659
Zr	1741
Mo	1590
Ba	1455
La	1578
Ce	1478
Nd	1602
Eu	1356
Hf	1684

In the following section, graphs display the abundance relative to solar vs T_C for each system. Two best-fit lines are calculated for each stellar data set: one using all elements, and another using only refractory ($T_C > 900K$) elements. The calculated linear functions for each relation are shown on the graphs, with the trendline slopes in units of $dex\ K^{-1}$.

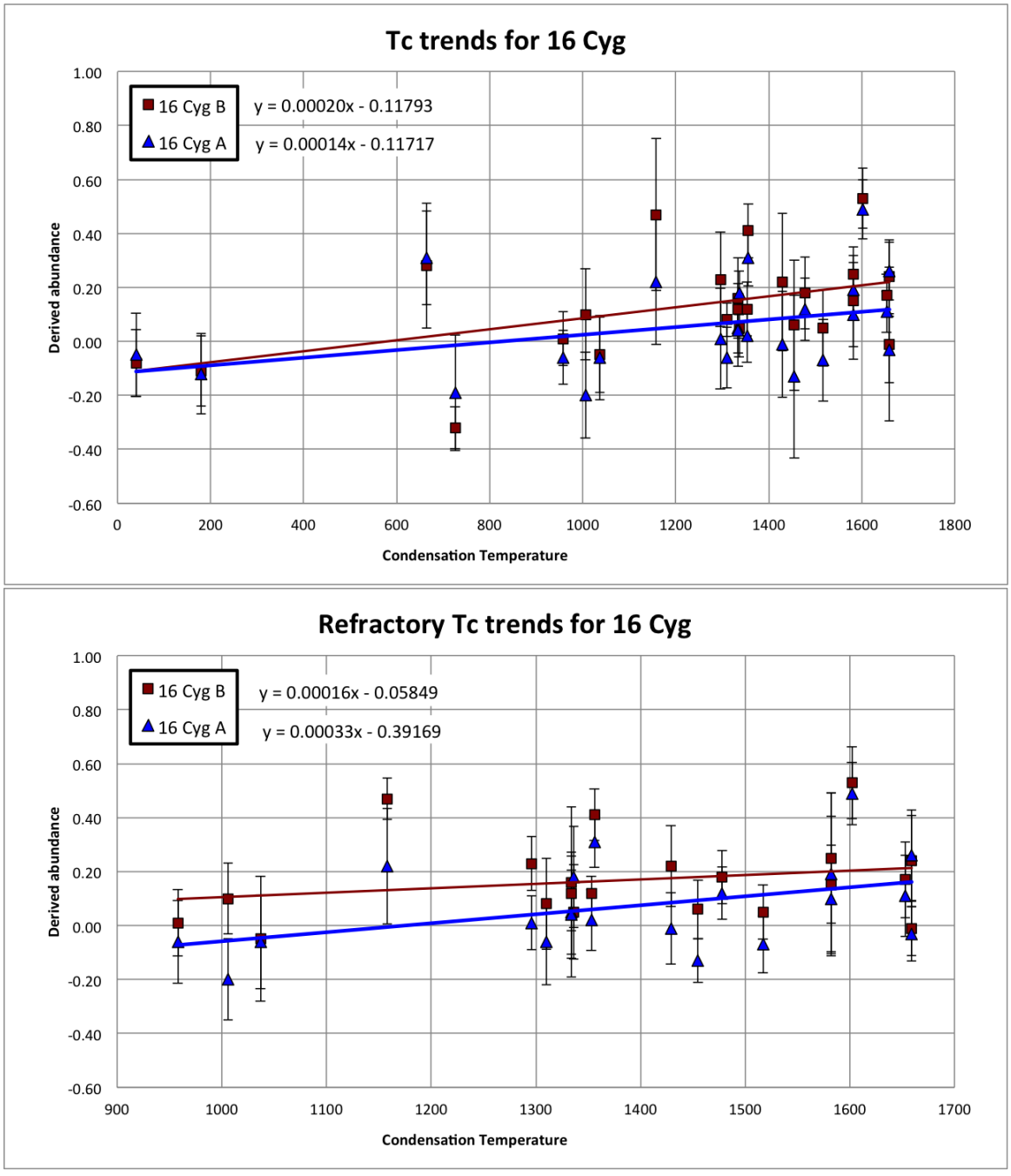

Figure 3.2: Abundances of 16 Cyg as a function of Condensation Temperature

Both components of 16 Cyg show a moderately positive slope in abundance vs T_C. This matches well with the overall result first reported by Schuler *et al.* (2011a), however the slopes here (16 and 33 $\times 10^{-5}$ dex K^{-1}, including all elements) are found to be greater than that study reported ($\sim 5 \times 10^{-5}$ dex K^{-1}) . Positive slopes in both systems indicate the likely lack of terrestrial planets, according to the arguments of Ramírez *et al.* (2010).

In the case of 16 Cyg B, a lack of terrestrial planets is in agreement with the high eccentricity and relatively close orbit of 16 Cyg Bb. A giant planet on an eccentric orbit would cause the orbits of small interior planets to by dynamically unstable. Terrestrial material forming interior to Bb would have been scattered and destroyed.

Both components of 83 Leo show high abundances of refractory elements, and solar to sub-solar abundances of volatile elements, giving them positive overall trends in abundance vs. T_C. The very positive slopes seen in these stars can be partially explained by their high overall metallicity. Galactic chemical evolution results in higher metallicity stars having lower [O/Fe] ratios (Ramírez *et al.*, 2007), which increases the overall slopes seen in abundance vs. T_C.

Accounting for only refractory elements, both components show negative T_C trends of similar magnitude. This depletion of high T_C elements may indicate that refractory material in this system was able to efficiently condense into dust (and later planets, where it remains sequestered), without being reaccreted onto the parent star. In the case of 83 Leo B, this material may be held in the cores of the two known sub-Jovian size planets, and perhaps in hitherto undiscovered smaller rocky planets.

Due to a low abundance of volatile elements, HD 109749 A has a positive overall trend of abundance vs. T_C trend. However, when accounting for only refractory elements, the trend of abundance vs. T_C becomes negative. This deficiency of the

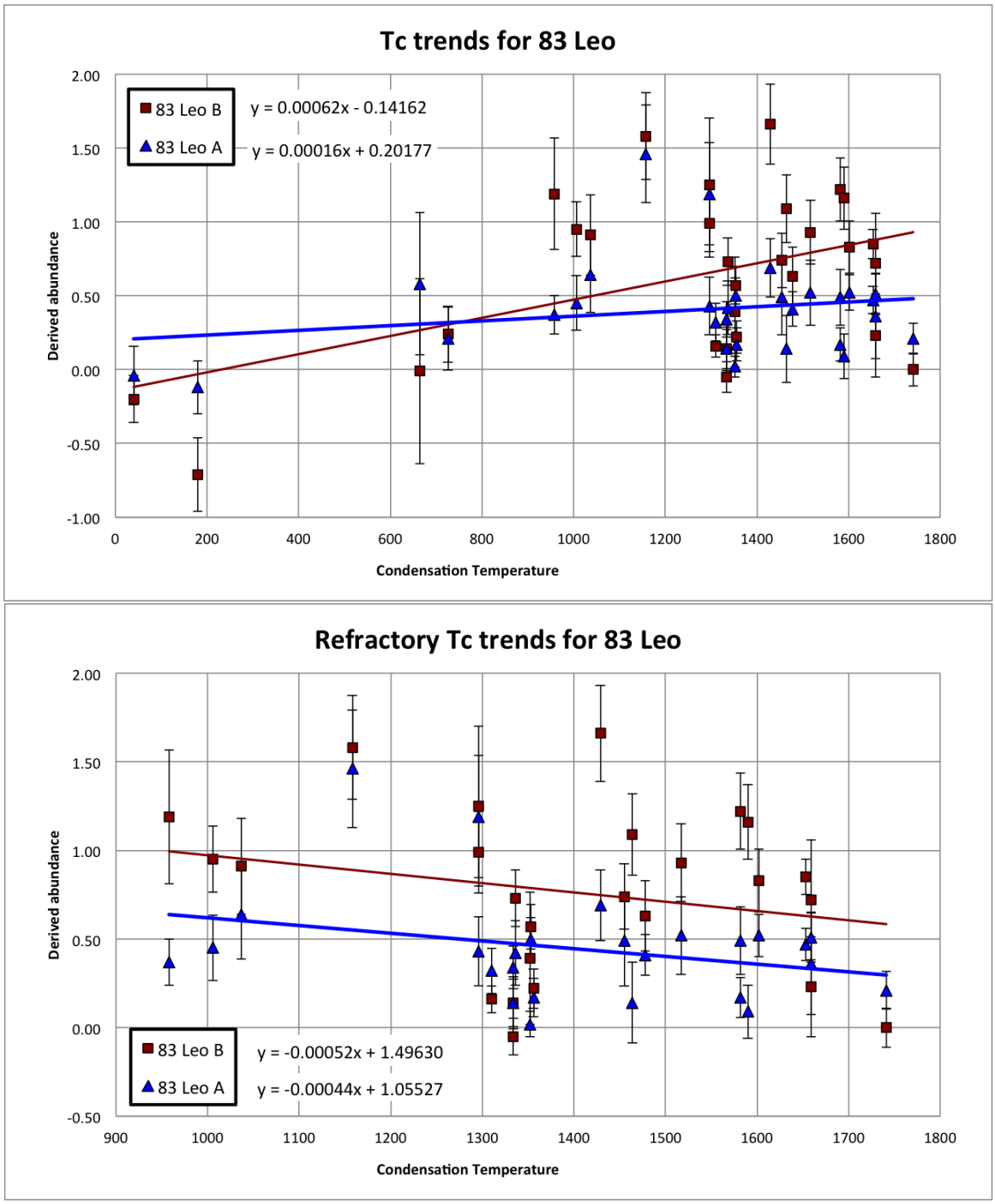

Figure 3.3: Abundances of 83 Leo as a function of Condensation Temperature

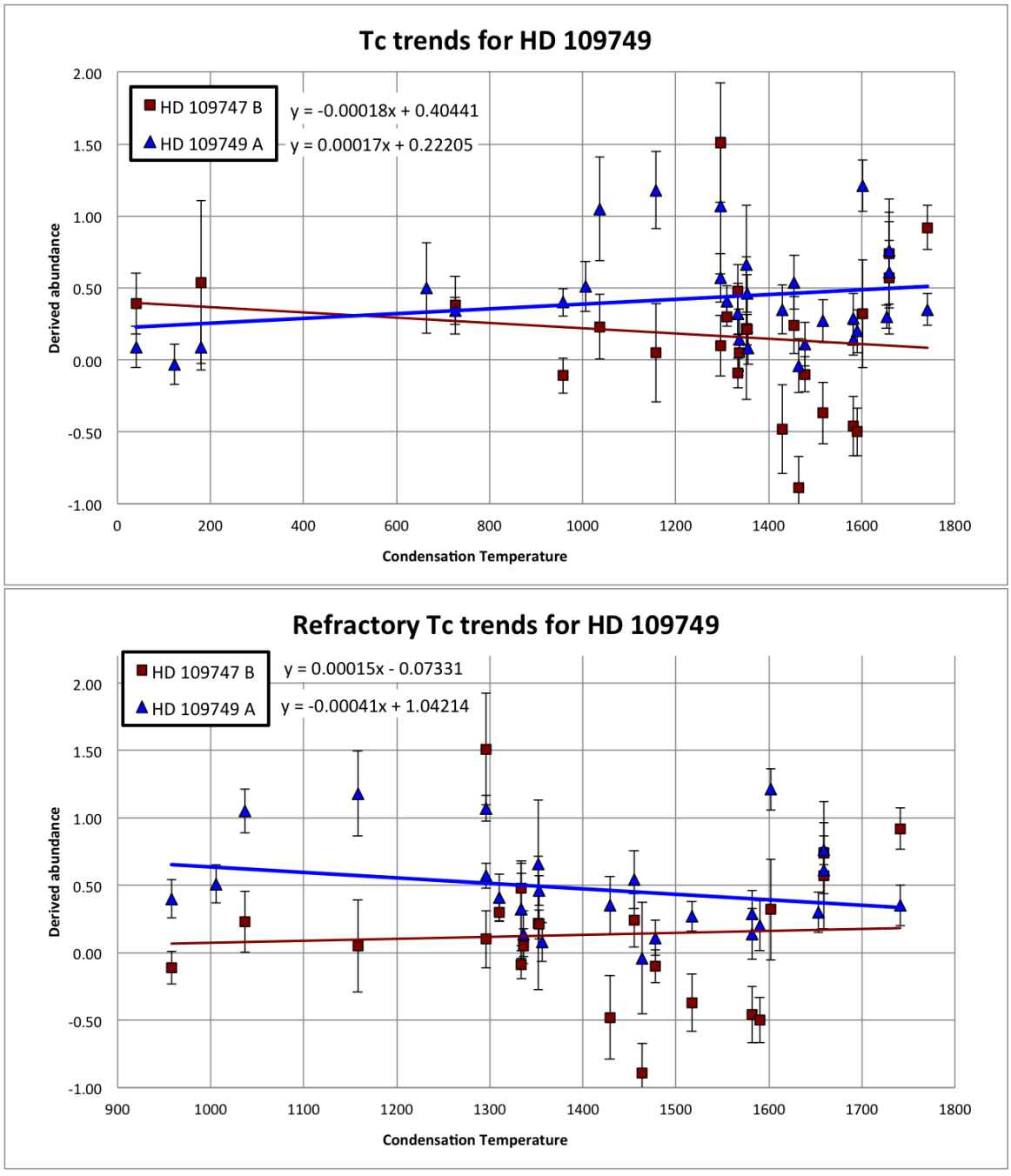

Figure 3.4: Abundances of HD 109749 as a function of Condensation Temperature

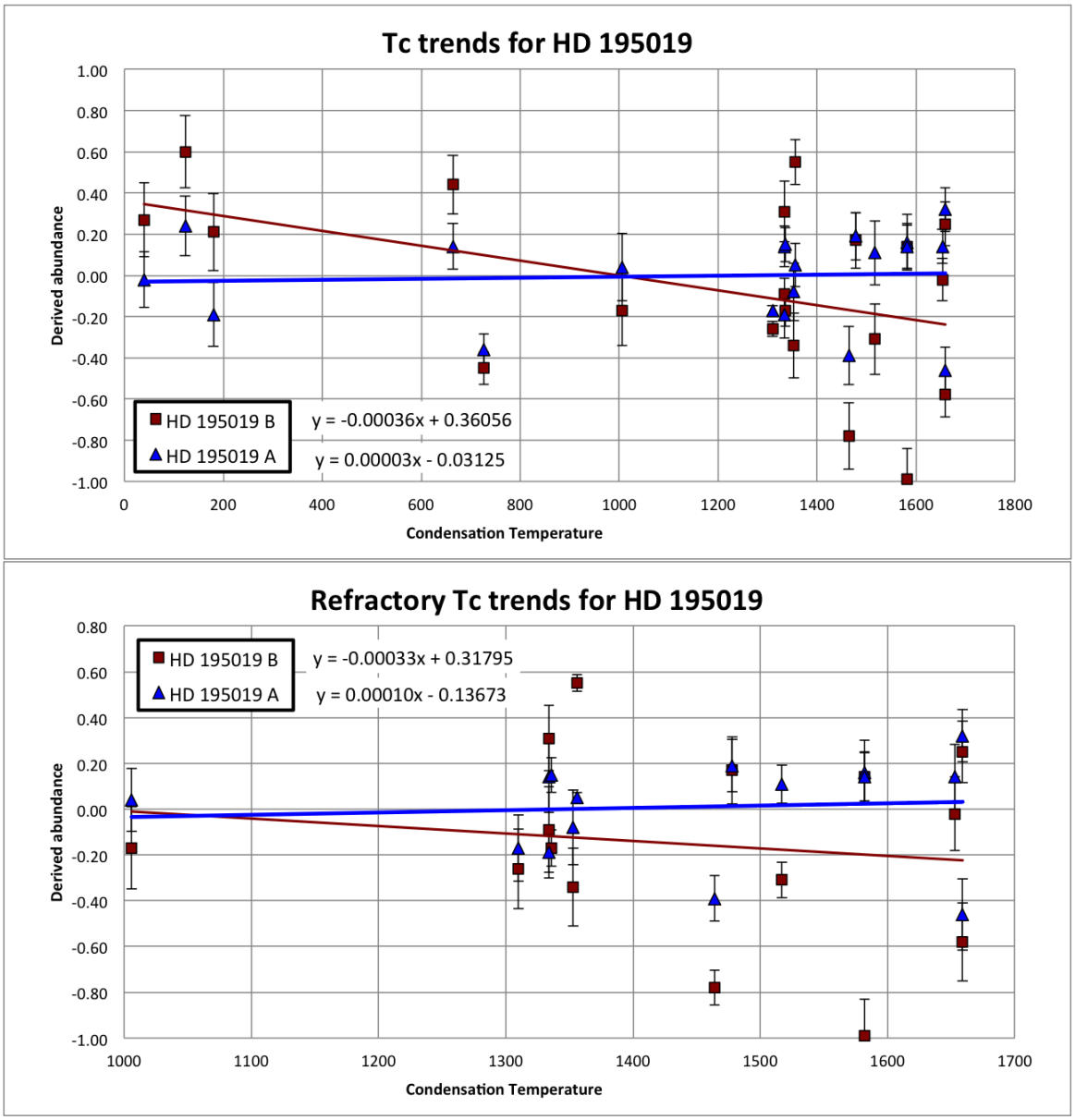

Figure 3.5: Abundances of HD 195019 as a function of Condensation Temperature

most refractory elements may indicate that the high T_C material is held in a planetary system. The B component shows a slight negative overall T_C trend, and a slight positive T_C trend for refractory elements, however the large spread between abundances of individual elements precludes any strong conclusions about potential planetary systems.

HD 195019A shows a small Tc trend with an overall slope of $3\times10^{-5} dex K^{-1}$ for all

elements, and a slightly larger 10 $\times 10^{-5} dex K^{-1}$ for only refractory elements. These values are in good agreement with those found by Schuler *et al.* (2011b), who report a refractory slope of 9.07 $\times 10^{-5} dex K^{-1}$ and give a similar self-enrichment explanation: given the fact that this star is host to a 3.7 Mj Hot-Jupiter planet at .14 AU, the slight enhancement in T_C elements may be due to inward planetary migration of early-formed refractory planetesimals and their subsequent accretion onto the star.

HD 195019B is found in both cases to have negative trends in T_C vs Abundance. In other systems, this has been hypothesized as a sign of terrestrial planet formation. Unfortunately the scatter in abundances is large and the correlation is very weak, so no strong conclusions should be made here.

3.3 Elemental Ratios

In a star, elements usually occur as a neutral or ionized gas, and while cooler stars do host some molecular species in their atmospheres, these molecules generally do not contribute to the overall structure or behavior of the star. However, in the case of planetary material, many elements exist as chemically processed compounds, minerals, and ices. It is the intrinsic physical properties of these resulting compounds and minerals which then give rise to the extrinsic properties of planetary cores, mantles, crusts, and atmospheres. Therefore, while elemental abundances may be considered the 'building blocks' of stars, condensed minerals may be a more appropriate conceptual building block for planets.

Specific minerals are defined by a set stoichiometric ratio of elements, so the resulting mineral (and therefore planetary) compositions in a planetary nebula are sensitive to the initial chemical compositions, particularly in terms of elemental ratios. While many planet-formation models have only relied on solar-system type compositions, Bond *et al.* (2010) carried out terrestrial planetary-formation simulations in

which the protoplanetary disc composition was a free input parameter. This study identified the Mg:Si and C:O ratio as key parameters determining the mineralogy of resulting terrestrial planets. Simulations of planetary formation using variable input compositions have been continued by Elser *et al.* (2012).

Table 3.3 gives the resulting C/O and Mg/Si ratios for each program star. The ratios are calculated by comparing the derived number density of each atomic species:

$$A/B = \frac{N_A}{N_B} = \frac{10^{Log(N_A)}}{10^{Log(N_B)}}$$

Also given are the upper and lower limits for each ratio, given the calculated uncertainty of each element (as given in Ch. 2). For example, to calculate the upper limit of C/O ratio, a star's uncertainty in C is added to its C abundance, while the uncertainty in O is subtracted from the O abundance, to yield the largest ratio possible within the given uncertainties. These upper and lower limits provide the error bars for Figure 3.6.

Table 3.3: Elemental Ratios

	C/O			Mg/Si		
Star	calculated	upper	lower	calculated	upper	lower
16 Cyg A	**0.501**	1.01	0.25	**1.862**	2.90	1.20
16 Cyg B	**0.457**	0.82	0.25	**1.000**	1.48	0.68
83 Leo A	**0.513**	1.22	0.22	**1.349**	2.75	0.66
83 Leo B	**1.380**	3.54	0.54	**3.981**	6.84	2.32
HD 109749 A	**0.427**	0.86	0.21	**0.575**	1.21	0.27
HD 109749 B	**0.302**	1.80	0.05	**0.603**	0.95	0.38
HD 195019 A	**0.631**	1.23	0.32	**2.239**	2.86	1.75
HD 195019 B	**0.490**	1.14	0.21	**1.318**	1.71	1.02

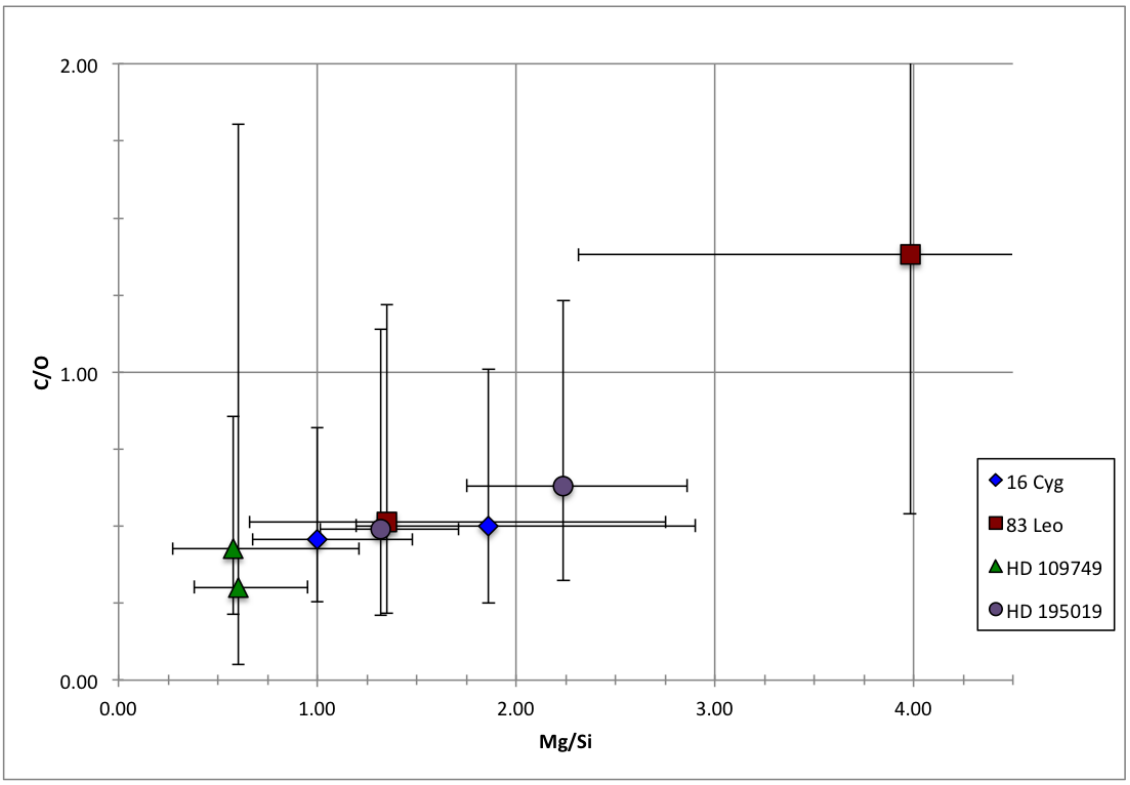

Figure 3.6: C/O ratio vs. Mg/Si ratio for each star

3.3.1 Carbon to Oxygen Ratio

The ratio of Carbon to Oxygen is one of the most important chemical metrics of an exoplanetary system, and has been the subject of numerous theoretical and observational studies. The C/O ratio of an exoplanet is determined partially by the initial composition of the protostellar nebula, as well as by the position within the protoplanetary disc that a planet forms (Öberg *et al.*, 2011).

The C/O ratio is a primary factor responsible for determining how silicon will be distributed between carbon and oxide species (Bond *et al.* (2010)). Due to differences in condensation pathways, there is thought to be a divide between a carbide-dominated and oxide (silicate) dominated chemical regimes, likely occurring around C/O ratios of 0.8. Systems with C/O ratios less than this will have silicate-dominated compositions akin to the solar system (having an estimated C/O ratio of 0.54 (Lod-

ders and Amari, 2005). Planets formed from higher C/O ratios could be dominated by carbide chemistry (SiC, graphite, and diamond being key mantle minerals), as suggested by Madhusudhan (2012). High C/O ratios have been observed in some transiting hot-Jupiter systems, inferred to have significant effects on atmospheric chemistry (Moses *et al.*, 2013).

Of the 8 stars analyzed in this study, 7 have C/O ratios below 0.8, with most falling near the Solar value of 0.54. Rocky planets in these systems are expected to have similar silicate chemistry to the solar system.

83 Leo B is found to be depleted in most volatiles, including Carbon ([C/H] =-0.20) and Oxygen ([O/H] = -0.71). This very low oxygen abundance yields a very high C/O ratio, nearly 1.4. However, the lower uncertainty limit on the C/O ratio of 83 Leo B is near solar, at 0.54. Furthermore, using the higher Oxygen abundance derived by Ecuvillon *et al.* (2006b) gives a lower C/O ratio, potentially below 0.8.

3.3.2 Magnesium to Silicon Ratio

In terrestrial planets, Iron and siderophile elements differentiate into a metallic core due to their high density. Most of the remaining material forms a rocky mantle, dominated by Magnesium and Silicon oxides. The mineral composition of this mantle is set from the available Magnesium to Silicon ratio, making this ratio an extremely important parameter in the resulting mantle properties of terrestrial planets. Olivine (Mg_2SiO_4) and Pyroxene ($MgSiO_3$) are two key silicate minerals in the earth's mantle. For systems with varying Mg/Si ratios, these minerals will occur in different proportions.

Based on models by Bond *et al.* (2010), systems with very high Mg/Si ratios (> 2) will form planets with almost entirely Olivine, and very low Mg/Si ratios will result in pyroxenes and feldspars. The sun has an intermediate Mg/Si ratio of 1.05,

corresponding to terrestrial planets dominated by pyroxene (and olivine) mineralogy. The stars in this study span Mg/Si ratios from near 0.5 to above 3.

16 Cyg B, well-known as a solar twin, is found here to have C/O (0.46) and Mg/Si (1.00) ratios indistinguishable from the sun. In HD 109749, both components have very similar C/O and Mg/Si ratios, so despite large variations in the abundances of some elements discussed earlier, the overall composition of hypothetical terrestrial planets in these systems is likely to be very similar. The planet-hosting HD195019 A is found to have a high Mg/Si ratio of 2.24.

Although 83 Leo A is found to have elemental ratios very close to the mean values of large stellar samples, 83 Leo B appears in this study to be a chemical outlier, with drastically different ratios than the other stars studied here. Even at the limits of its large uncertainty, 83 Leo B has very high C/O and Mg/Si ratios as compared to the other stars in this sample, as well as to samples from other studies. These values make the planets in 83 Leo B very strong candidates for Carbon planets, which would also contain nearly all their silicon in the form of Olivine (with nearly no Pyroxene present).

3.4 System Architectures

Although all the systems in this study have two main stellar components, their stellar architectures and planetary systems display a range of properties. 16 Cyg is in fact likely a triple system (Patience *et al.*, 2002), including a M dwarf companion in a close orbit around 16 Cyg A at 22 AU. Physical properties of each stellar system are reiterated in Table 3.4. Separation distances are given from the A component of the system.

The systems HD 109749 and 195019 are similar in terms of several properties. Both systems have a planet-hosting G-type primary, accompanied by a K-type sec-

Table 3.4: Stellar and Planetary properties

System	Stellar properties			Planet properties		
	Comp.	Sp. type	Separation (AU)	a (AU)	Msin(i) (M_{Jup})	e
	B	G3V	860	1.68	1.5	0.63
16 Cyg	A	G1.5Vb		-	-	-
	C	M	22	-	-	-
HD 109749	A	G3V		0.06	0.28	0.01
	B	K5V	496	-	-	-
HD 195019	A	G1V		0.14	3.7	0.03
	B	K3	150	-	-	-
83 Leo	B	K2V	589	0.123	0.109	0.254
				5.4	0.36	0.106
	A	K0IV				

ondary with no detected planets. Furthermore, both planetary systems are composed of one massive planet, close-in planet, on a nearly circular orbit. Formation of these "hot Jupiters" almost certainly occurred at much larger orbital distances, after which the planets experienced inward migration to their present orbits. This process would have resulted in the host stars re-accreting a large amount of initial protoplanetary disc material. Evidence for this has been observed as a positive $[m/H]$ vs T_C trend for refractory elements, in HD195109A by Schuler *et al.* (2011b) and confirmed here for both stars. This putative re-accretion trend is more pronounced in HD109749, which also has a much smaller (super-neptune size) planet of 0.28 Mj. One possible explanation is that the HD195019A system has sequestered more of its refractory material its larger planet.

A major difference between the systems is the orbital separation between stellar components, being 3.3 times larger in HD109749. The binary companion of a planet-forming system is expected to truncate the protoplanetary disc, with increasing effect at close orbital distances. Given these two (otherwise similar) systems, it is therefore surprising that the smaller planet is found in the system with wider stellar components.

16 Cyg is the most self-similar system in this study - the two main components are both "solar twins", G type stars with similar properties and compositions to the sun. The A and B components have been found (both in this study and by others) to be nearly indistinguishable in stellar parameters and elemental composition (other than the case of Li), with most measurements falling within mutual uncertainties. One of the major differences between the stars is the known planetary system of 16 Cyg B, and the lack of known planets around 16 Cyg A. However, 16 Cyg A *does* have an orbiting companion object - the M dwarf 16 Cyg C. The existence and proximity (22 AU) of 16 Cyg C may provide a reason that no (large) planets exist around 16 Cyg A: tidal disturbances from 16 Cyg C may have prevented (or impeded) the formation of any large objects in 16 Cyg A's protoplanetary disc.

The two components of 83 Leo are both K-type stars, however they differ in their evolutionary stage. The A component is a K0IV subgiant star, while the planet-hosting B star is a main-sequence K2V. This system is the only multi-planet system in our study, with two sub-jovian planets of Msin(i) = 0.109 and 0.36 Mj.

Based on the negative trend in abundance vs. condensation temperature for 83 Leo B (described earlier), it may be argued that the observed depletion of higher T_C elements is a sign of refractory material sequestered in the planetary system. While the two known planets are too large to be terrestrial worlds, it is possible that they contain large refractory-rich cores. Undiscovered smaller planets could also contain

significant amounts of refractory material. By contrast, the more evolved 83 Leo A has no known planets. Given the star's very high metallicity, it is quite likely that at some point 83 Leo A harbored a planetary system. One possibility is that a close-in planetary system did develop around 83 Leo A, but was much later re-accreted into the star as it underwent post main-sequence evolution into a subgiant. This possibility would fit with the very positive $[m/H]$ vs T_C trend observed in the star.

3.5 Concluding remarks

In this research, stellar abundances have been analyzed for 4 binary systems, and interpreted with regards to the exoplanets in each system. Looking at stellar elemental compositions over a wide suite of elements helps to give an overall view of the system, especially when comparing the exoplanet host star to its non-host binary companion. The strongest single-element trend found in this study is that of Sr, which was found in greater quantities in every Exoplanet host as compared to its binary companion.

In general, it is found that the chemical similarity of the binaries studied here matches well with the similarity of their spectral types. In the system having the most chemically similar components, 16 Cyg, both components also have very similar spectral types (G1.5V and G3V). The systems HD109749 and HD195019 have binary components of disparate masses (each with a G-type and K-type component), and also have compositions that differ from each other more significantly.

While this study cannot directly determine the composition of individual planets, it does place some constrains on system-wide composition of the 4 binary systems. Most of the stars in this study have C/O and Mg/Si ratios within the "normal" (according to solar-system composition) range. Rocky planets, if they exist in these systems, would be dominated by Silicate minerals with an intermediate Olivine/Pyroxene mix.

83 Leo B is found to have an exotic composition. This system has known planets with orbits of 1.23 and 5.4 AU, placing one inside and one outside the star's expected Habitable zone. The host star is found to have a composition with extremely high Mg/Si and C/O ratios, as well as being relatively depleted in the more refractory elements. This indicates that 83 Leo's planets have a large refractory budget, and that the system's rocky material is carbide-dominated. Such planets, with large cores and carbide mantles (as well as Carbon-rich atmospheres), would be extremely unlike any in our solar system.

3.5.1 Future work

This type of abundance analysis would benefit from several advances, both in the methodologies applied here (which were limited by the duration of this study), as well as in terms of a wider theoretical framework. The methods used in this study would be much improved with a more streamlined data processing pipeline. Especially beneficial would be an automated iterative program to more fully explore the parameter space of stellar atmospheres, which would allow for more accurate stellar parameters. Furthermore, as demonstrated by Figure **??**, more work can be done to improve the agreement of ARES and splot measurements of Equivalent Widths. Finally, given the fact that multiple HIRES observations of each target are needed for RV surveys, it may be beneficial to perform the entire abundance analysis on multiple datasets for a single star. The average abundance from all observations could then be used, and the spread in these measurements could give an additional uncertainty quantification.

In connecting the composition of a Host star with that of its planets, more detailed models are needed to simulate composition-dependent condensation and planetary formation. Work such as Bond *et al.* (2010) has begun to address this question, but

significant work remains to be done in analyzing the detailed effects on planetary formation and dynamics of non-solar compositions. One especially relevant point can be seen in the many studies (including this one) connecting published condensation temperatures (such as from Lodders (2003)) with trends in systems of varying compositions. The published elemental condensation temperatures are those of the minerals that would form given a solar composition. However, for systems deviating from solar composition, the condensation pathways would be different, resulting in elements condensing into different minerals *at different temperatures*. Published elemental condensation temperatures assume a composition - if composition is meant to be a variable of study, then the entire condensation sequence should be recalculated for that composition.

Given better models to connect host star and planet composition, stellar abundance analyses such as this will provide an easily-obtainable wealth of chemical information, thereby revealing the broad diversity of system and planetary compositions present in our galaxy.

REFERENCES

Allen, C., A. Poveda and M. A. Herrera, "Wide binaries among high-velocity and metal-poor stars", Astronomy and Astrophysics **356**, 529–540 (2000).

Ammann, M. W., J. P. Brodholt and D. P. Dobson, "Ferrous iron diffusion in ferropericlase across the spin transition", Earth and Planetary Science Letters **302**, 3-4, 393–402 (2011).

Anders, E. and N. Grevesse, "Abundances of the elements - Meteoritic and solar", Geochimica et Cosmochimica Acta (ISSN 0016-7037) **53**, 197–214 (1989).

Arnett, D., *Supernovae and Nucleosynthesis: An Investigation of the History of Matter, from the Big Bang to the Present* (1996).

Asplund, M., "New light on stellar abundance analyses: departures from LTE and homogeneity", Annual Review of Astronomy and Astrophysics **43**, 481–530 (2005).

Beirão, P., N. C. Santos, G. Israelian and M. Mayor, "Abundances of Na, Mg and Al in stars with giant planets", Astronomy and Astrophysics **438**, 1, 251–256 (2005).

Bodaghee, A., N. C. Santos, G. Israelian and M. Mayor, "Chemical abundances of planet-host stars", Astronomy and Astrophysics **404**, 2, 715–727 (2003).

Bond, J. C., D. P. O'Brien and D. S. Lauretta, "THE COMPOSITIONAL DIVERSITY OF EXTRASOLAR TERRESTRIAL PLANETS. I. IN SITU SIMULATIONS", The Astrophysical Journal Letters **715**, 2, 1050–1070 (2010).

Bord, P., D. Rouan and A. L ger, "Exoplanet detection capability of the COROT space mission", Astronomy and Astrophysics **405**, 3, 1137–1144 (2003).

Borucki, W., D. Koch, N. Batalha, D. Caldwell, J. Christensen-Dalsgaard, W. D. Cochran, E. Dunham, T. N. Gautier, J. Geary, R. Gilliland, J. Jenkins, H. Kjeldsen, J. J. Lissauer and J. Rowe, "KEPLER: Search for Earth-Size Planets in the Habitable Zone", Transiting Planets **253**, 289–299 (2009).

Boss, A. P., "Giant Planet Formation by Gravitational Instability", Science **276**, 5320, 1836–1839 (1997).

Boss, A. P., "Formation of Giant Planets by Disk Instability on Wide Orbits Around Protostars with Varied Masses", The Astrophysical Journal **731**, 1, 74 (2011).

Brugamyer, E., S. E. Dodson-Robinson, W. D. Cochran and C. Sneden, "SILICON AND OXYGEN ABUNDANCES IN PLANET-HOST STARS", The Astrophysical Journal Letters **738**, 1, 97 (2011).

Bubar, E. J. and J. R. King, "SPECTROSCOPIC ABUNDANCES AND MEMBERSHIP IN THE WOLF 630 MOVING GROUP", The Astronomical Journal **140**, 2, 293–318 (2010).

Carolo, E., S. Desidera, R. Gratton, A. M. Fiorenzano, M. Endl, R. Cosentino, M. Barbieri, M. Bonavita, M. Cecconi, R. Claudi, F. Marzari and S. Scuderi, "Planet candidates from the SARG visual binary survey", The Astrophysics of Planetary Systems: Formation **276**, 403–404 (2011).

Chauvin, G., A. M. Lagrange, S. Udry, T. Fusco, F. Galland, D. Naef, J. L. Beuzit and M. Mayor, "Probing long-period companions to planetary hosts. VLT and CFHT near infrared coronographic imaging surveys", Astronomy and Astrophysics **456**, 3, 1165–1172 (2006).

Cochran, W. D., A. P. Hatzes, R. P. Butler and G. W. Marcy, "The Discovery of a Planetary Companion to 16 Cygni B", arXiv.org (1996).

de Koker, N., B. B. Karki and L. Stixrude, "Thermodynamics of the MgO-SiO2 liquid system in Earth's lowermost mantle from first principles", Earth and Planetary Science Letters **361**, 58–63 (2013).

Delgado Mena, E., G. Israelian, J. I. González Hernández, J. C. Bond, N. C. Santos, S. Udry and M. Mayor, "CHEMICAL CLUES ON THE FORMATION OF PLANETARY SYSTEMS: C/O VERSUS Mg/Si FOR HARPS GTO SAMPLE", The Astrophysical Journal Letters **725**, 2, 2349–2358 (2010).

Desidera, S. and M. Barbieri, "Properties of planets in binary systems", Astronomy and Astrophysics **462**, 1, 345–353 (2007).

Duchene, G., "Planet formation in binary systems: A separation-dependent mechanism?", The Astrophysical Journal Letters **709**, 2, L114 (2010).

Duquennoy, A. and M. Mayor, "Multiplicity among solar-type stars in the solar neighbourhood. II - Distribution of the orbital elements in an unbiased sample", Astronomy and Astrophysics (ISSN 0004-6361) **248**, 485–524 (1991).

Ebel, D. S., "Condensation of Rocky Material in Astrophysical Environments", in "Meteorites and the Early Solar System II", pp. 253–277 (Meteorites and the Early Solar System II, 2006).

Ebel, D. S. and L. Grossman, "Condensation in dust-enriched systems", Geochimica et Cosmochimica Acta **64**, 2, 339–366 (2000).

Ecuvillon, A., G. Israelian, N. C. Santos, M. Mayor and G. Gilli, "Abundance ratios of volatile vs. refractory elements in planet-harbouring stars: hints of pollution?", Astronomy and Astrophysics **449**, 2, 809–816 (2006a).

Ecuvillon, A., G. Israelian, N. C. Santos, N. G. Shchukina, M. Mayor and R. Rebolo, "Oxygen abundances in planet-harbouring stars", Astronomy and Astrophysics **445**, 2, 633–645 (2006b).

Eggenberger, A., S. Udry and M. Mayor, "Statistical properties of exoplanets. III. Planet properties and stellar multiplicity", Astronomy and Astrophysics **417**, 353–360 (2004).

Elser, S., M. R. Meyer and B. Moore, "On the origin of elemental abundances in the terrestrial planets", arXiv.org (2012).

Favata, F., G. Micela and S. Sciortino, "Lithium abundance in a volume-limited sample of nearby main sequence G and K stars.", Astronomy and Astrophysics **311**, 951–960 (1996).

Feltzing, S. and G. Gonzalez, "The nature of super-metal-rich stars", Astronomy and Astrophysics **367**, 1, 253–265 (2001).

Fischer, D. A., G. Laughlin, G. W. Marcy, R. P. Butler, S. S. Vogt, J. A. Johnson, G. W. Henry, C. McCarthy, M. Ammons, S. Robinson, J. Strader, J. A. Valenti, P. R. McCullough, D. Charbonneau, J. Haislip, H. A. Knutson, D. E. Reichart, P. McGee, B. Monard, J. T. Wright, S. Ida, B. Sato and D. Minniti, "The N2K Consortium. III. Short-Period Planets Orbiting HD 149143 and HD 109749", The Astrophysical Journal **637**, 2, 1094–1101 (2006).

Fischer, D. A., G. W. Marcy, R. P. Butler, S. S. Vogt and K. Apps, "Planetary Companions around Two SolarType Stars: HD 195019 and HD 217107", Publications of the Astronomical Society of the Pacific **111**, 755, 50–56 (1999).

Fischer, D. A. and J. Valenti, "The Planet-Metallicity Correlation", The Astrophysical Journal **622**, 2, 1102–1117 (2005).

Gálvez-Ortiz, M. C., E. Delgado Mena, J. I. González Hernández, G. Israelian, N. C. Santos, R. Rebolo and A. Ecuvillon, "Beryllium abundances in stars with planets", Astronomy and Astrophysics **530**, A66 (2011).

Gilli, G., G. Israelian, A. Ecuvillon, N. C. Santos and M. Mayor, "Abundances of refractory elements in the atmospheres of stars with extrasolar planets", Astronomy and Astrophysics **449**, 2, 723–736 (2006).

Gonzalez, G., "The stellar metallicity-giant planet connection", Monthly Notices of the Royal Astronomical Society **285**, 403–412 (1997).

Gonzalez, G., "Spectroscopic analyses of the parent stars of extrasolar planetary system candidates", Astronomy and Astrophysics **334**, 221–238 (1998).

Gonzalez, G., M. K. Carlson and R. W. Tobin, "Parent stars of extrasolar planets - XI. Trends with condensation temperature revisited", Monthly Notices of the Royal Astronomical Society **407**, 1, 314–320 (2010).

Gratton, R., E. Carretta, R. U. Claudi, S. Desidera, S. Lucatello, G. Bonanno, R. Cosentino, S. Scuderi, M. Barbieri, F. Marzari, M. Endl, E. Brocato, M. Dolci and G. Valentini, "The SARG Planet Search: Hunting for Planets Around Stars in Wide Binaries", Scientific Frontiers in Research on Extrasolar Planets **294**, 47–50 (2003).

Guillot, T., N. C. Santos, F. Pont, N. Iro, C. Melo and I. Ribas, "A correlation between the heavy element content of transiting extrasolar planets and the metallicity of their parent stars", arXiv.org , 2, L21–L24 (2006).

Haghighipour, N., R. Dvorak and E. Pilat-Lohinger, "Planetary Dynamics and Habitable Planet Formation In Binary Star Systems", in "Planets in Binary Star Systems", edited by N. Haghighipour (arXiv.org, 2009).

Han, I., D. C. Black and G. Gatewood, "Preliminary Astrometric Masses for Proposed Extrasolar Planetary Companions", The Astrophysical Journal **548**, 1, L57–L60 (2001).

Hatzes, A. P., W. D. Cochran and M. Endl, "The Detection of Extrasolar Planets Using Precise Stellar Radial Velocities", Planets in Binary Star Systems **366**, 51 (2010).

Hauser, H. M. and G. W. Marcy, "The Orbit of 16 Cygni AB", Publications of the Astronomical Society of the Pacific **111**, 757, 321–334 (1999).

Heiter, U. and R. E. Luck, "Abundance Analysis of Planetary Host Stars I. Differential Iron Abundances", arXiv.org (2003).

Hough, G. W., "Catalogue of 209 New Double Stars", Astronomische Nachrichten **116**, 273 (1887).

Ida, S. and D. Lin, "Toward a deterministic model of planetary formation. IV. Effects of type I migration", The Astrophysical Journal Letters **673**, 1, 487 (2008).

Ida, S. and D. N. C. Lin, "Toward a Deterministic Model of Planetary Formation. II. The Formation and Retention of Gas Giant Planets around Stars with a Range of Metallicities", The Astrophysical Journal **616**, 1, 567–572 (2004).

Johnson, J. A. and K. Apps, "ON THE METAL RICHNESS OF M DWARFS WITH PLANETS", The Astrophysical Journal Letters **699**, 2, 933–937 (2009).

Kaib, N. A., S. N. Raymond and M. Duncan, "Planetary system disruption by Galactic perturbations to wide binary stars", Nature **493**, 7432, 381–384 (2013).

Kang, W., S.-G. Lee and K.-M. Kim, "ABUNDANCES OF REFRACTORY ELEMENTS FOR G-TYPE STARS WITH EXTRASOLAR PLANETS", The Astrophysical Journal Letters **736**, 2, 87 (2011).

Kokubo, E. and S. Ida, "Formation of protoplanet systems and diversity of planetary systems", The Astrophysical Journal Letters **581**, 1, 666 (2002).

Konacki, M., "The Radial Velocity Search for Extrasolar Planets in Binary and Multiple Stellar Systems", American Astronomical Society Meeting 207 **207**, 1310 (2005).

Kurucz, R., "ATLAS9 Stellar Atmosphere Programs and 2 km/s grid.", ATLAS9 Stellar Atmosphere Programs and 2 km/s grid. Kurucz CD-ROM No. 13. Cambridge **13** (1993).

Lodders, K., "Solar System Abundances and Condensation Temperatures of the Elements", The Astrophysical Journal Letters **591**, 2, 1220–1247 (2003).

Lodders, K. and S. Amari, "Presolar grains from meteorites: Remnants from the early times of the solar system", Chemie der Erde - Geochemistry **65**, 93–166 (2005).

Madhusudhan, N., "C/O Ratio as a Dimension for Characterizing Exoplanetary Atmospheres", The Astrophysical Journal **758**, 1, 36 (2012).

Madhusudhan, N., O. Mousis, T. V. Johnson and J. I. Lunine, "Carbon-rich Giant Planets: Atmospheric Chemistry, Thermal Inversions, Spectra, and Formation Conditions", The Astrophysical Journal Letters **743**, 191 (2011).

Marcy, G. W., R. P. Butler, S. S. Vogt, D. A. Fischer, G. W. Henry, G. Laughlin, J. T. Wright and J. A. Johnson, "Five New Extrasolar Planets", The Astrophysical Journal Letters **619**, 1, 570–584 (2005).

Matsuo, T., H. Shibai, T. Ootsubo and M. Tamura, "Planetary Formation Scenarios Revisited: CoreAccretion versus Disk Instability", The Astrophysical Journal Letters **662**, 2, 1282–1292 (2007).

Meléndez, J., M. Asplund, B. Gustafsson and D. Yong, "The Peculiar Solar Composition and Its Possible Relation to Planet Formation", The Astrophysical Journal Letters **704**, L66 (2009).

Meschiari, S., G. Laughlin, S. S. Vogt, R. P. Butler, E. J. Rivera, N. Haghighipour and P. Jalowiczor, "THE LICK-CARNEGIE SURVEY: FOUR NEW EXOPLANET CANDIDATES", The Astrophysical Journal Letters **727**, 2, 117 (2011).

Mordasini, C., Y. Alibert, W. Benz and D. Naef, "Giant Planet Formation by Core Accretion", arXiv.org (2007).

Moses, J. I., N. Madhusudhan, C. Visscher and R. S. Freedman, "Chemical Consequences of the C/O Ratio on Hot Jupiters: Examples from WASP-12b, CoRoT-2b, XO-1b, and HD 189733b", The Astrophysical Journal **763**, 1, 25 (2013).

Moutou, C., F. Pont, F. Bouchy and M. Mayor, "Accurate radius and mass of the transiting exoplanet OGLE-TR-132b", Astronomy and Astrophysics **424**, 3, L31–L34 (2004).

Mugrauer, M., R. Neuhäuser, T. Mazeh, E. Guenther, M. Fernández and C. Broeg, "A search for wide visual companions of exoplanet host stars: The Calar Alto Survey", Astronomische Nachrichten **327**, 4, 321 (2006).

Muterspaugh, M. W., M. Konacki, B. F. Lane and E. Pfahl, "Observational Techniques for Detecting Planets in Binary Systems", in "Planets in Binary Star Systems", edited by N. Haghighipour, p. 3072 (arXiv.org, 2007).

Muterspaugh, M. W., B. F. Lane, S. R. Kulkarni, M. Konacki, B. F. Burke, M. M. Colavita, M. Shao, W. I. Hartkopf, A. P. Boss and M. Williamson, "THE PHASES DIFFERENTIAL ASTROMETRY DATA ARCHIVE. V. CANDIDATE SUBSTELLAR COMPANIONS TO BINARY SYSTEMS", The Astronomical Journal **140**, 6, 1657–1671 (2010).

Öberg, K. I., R. Murray-Clay and E. A. Bergin, "The Effects of Snowlines on C/O in Planetary Atmospheres", The Astrophysical Journal Letters **743**, 1, L16 (2011).

Oppenheimer, B. R., C. Baranec, C. Beichman, D. Brenner, R. Burruss, E. Cady, J. R. Crepp, R. Dekany, R. Fergus, D. Hale, L. Hillenbrand, S. Hinkley, D. W. Hogg, D. King, E. R. Ligon, T. Lockhart, R. Nilsson, I. R. Parry, L. Pueyo, E. Rice, J. E. Roberts, L. C. R. Jr, M. Shao, A. Sivaramakrishnan, R. Soummer, T. Truong, G. Vasisht, A. Veicht, F. Vescelus, J. K. Wallace, C. Zhai and N. Zimmerman, "Reconnaissance of the HR 8799 Exosolar System I: Near IR Spectroscopy", arXiv **astro-ph.EP** (2013).

Patience, J., R. J. White, A. M. Ghez, C. McCabe, I. S. McLean, J. E. Larkin, L. Prato, S. S. Kim, J. P. Lloyd, M. C. Liu, J. R. Graham, B. A. Macintosh, D. T. Gavel, C. E. Max, B. J. Bauman, S. S. Olivier, P. Wizinowich and D. S. Acton, "Stellar Companions to Stars with Planets", The Astrophysical Journal Letters **581**, 1, 654–665 (2002).

Perryman, M., *The Exoplanet Handbook* (Cambridge University Press, 2011).

Petigura, E. A. and G. W. Marcy, "CARBON AND OXYGEN IN NEARBY STARS: KEYS TO PROTOPLANETARY DISK CHEMISTRY", The Astrophysical Journal Letters **735**, 1, 41 (2011).

Raghavan, D., T. J. Henry, B. D. Mason, J. P. Subasavage, W.-C. Jao, T. D. Beaulieu and N. C. Hambly, "Two Suns in The Sky: Stellar Multiplicity in Exoplanet Systems", The Astrophysical Journal Letters **646**, 1, 523–542 (2006).

Rameau, J., G. Chauvin, A. M. Lagrange, A. Boccaletti, S. P. Quanz, M. Bonnefoy, J. H. Girard, P. Delorme, S. Desidera, H. Klahr, C. Mordasini, C. Dumas, M. Bonavita, T. Meshkat, V. Bailey and M. Kenworthy, "Discovery of a probable 4-5 Jupiter-mass exoplanet to HD 95086 by direct-imaging", (2013).

Ramírez, I., C. Allende Prieto and D. L. Lambert, "Oxygen abundances in nearby stars. Clues to the formation and evolution of the Galactic disk", Astronomy and Astrophysics **465**, 1, 271–289 (2007).

Ramírez, I., M. Asplund, P. Baumann, J. Meléndez and T. Bensby, "A possible signature of terrestrial planet formation in the chemical composition of solar analogs", Astronomy and Astrophysics **521**, A33 (2010).

Ramírez, I., J. Meléndez and M. Asplund, "Accurate abundance patterns of solar twins and analogs. Does the anomalous solar chemical composition come from planet formation?", Astronomy and Astrophysics **508**, 1, L17–L20 (2009).

Ramírez, I., J. Meléndez, D. Cornejo, I. U. Roederer and J. R. Fish, "ELEMENTAL ABUNDANCE DIFFERENCES IN THE 16 CYGNI BINARY SYSTEM: A SIGNATURE OF GAS GIANT PLANET FORMATION?", The Astrophysical Journal Letters **740**, 2, 76 (2011).

Rice, K., M. T. Penny and K. Horne, "How fast do Jupiters grow? Signatures of the snowline and growth rate in the distribution of gas giant planets", arXiv.org (2012).

Robinson, S. E., G. Laughlin, P. Bodenheimer and D. Fischer, "Silicon and Nickel Enrichment in Planet Host Stars: Observations and Implications for the Core Accretion Theory of Planet Formation", The Astrophysical Journal Letters **643**, 1, 484–500 (2006).

Roell, T., A. Seifahrt, R. Neuhäuser and M. Mugrauer, "Extrasolar planets in stellar multiple systems", arXiv.org (2012).

Santos, N. C., G. Israelian and M. Mayor, "The metal-rich nature of stars with planets", Astronomy and Astrophysics **373**, 3, 1019–1031 (2001).

Santos, N. C., G. Israelian, M. Mayor, J. P. Bento, P. C. Almeida, S. G. Sousa and A. Ecuvillon, "Spectroscopic metallicities for planet-host stars: Extending the samples", Astronomy and Astrophysics **437**, 3, 1127–1133 (2005).

Santos, N. C., G. Israelian, M. Mayor, R. Rebolo and S. Udry, "Statistical properties of exoplanets", Astronomy and Astrophysics **398**, 1, 363–376 (2003).

Schuler, S. C., K. Cunha, V. V. Smith, L. Ghezzi, J. R. King, C. P. Deliyannis and A. M. Boesgaard, "DETAILED ABUNDANCES OF THE SOLAR TWINS 16 CYGNI A AND B: CONSTRAINING PLANET FORMATION MODELS", The Astrophysical Journal **737**, 2, L32 (2011a).

Schuler, S. C., D. Flateau, K. Cunha, J. R. King, L. Ghezzi and V. V. Smith, "ABUNDANCES OF STARS WITH PLANETS: TRENDS WITH CONDENSATION TEMPERATURE,", The Astrophysical Journal Letters **732**, 1, 55 (2011b).

Smith, V. V., K. Cunha and D. Lazzaro, "The Abundance Distribution in the Extrasolar-Planet Host Star HD 19994", The Astronomical Journal **121**, 6, 3207 (2001).

Sneden, C., "The nitrogen abundance of the very metal-poor star HD 122563.", Astrophysical Journal **184**, 839–849 (1973).

Sousa, S. G., N. C. Santos, G. Israelian, M. Mayor and M. J. P. F. G. Monteiro, "Spectroscopic parameters for a sample of metal-rich solar-type stars", Astronomy and Astrophysics **458**, 3, 873–880 (2006).

Sousa, S. G., N. C. Santos, G. Israelian, M. Mayor and M. J. P. F. G. Monteiro, "A new code for automatic determination of equivalent widths: Automatic Routine for line Equivalent widths in stellar Spectra (ARES)", Astronomy and Astrophysics **469**, 2, 783–791 (2007).

Takeda, G., E. B. Ford, A. Sills, F. A. Rasio, D. A. Fischer and J. A. Valenti, "Structure and Evolution of Nearby Stars with Planets. II. Physical Properties of 1000 Cool Stars from the SPOCS Catalog", Astrophysical Journal Supplement Series **168**, 2, 297–318 (2007).

Takeda, Y., "Fundamental Parameters and Elemental Abundances of 160 FGK Stars Based on OAO Spectrum Database", Publications of the Astronomical Society of Japan **59**, 335–356 (2007).

Turner, N. H., A. Theo, H. A. Mcalister, B. D. Mason, W. I. Hartkopf and L. C. Roberts, Jr, "Search for Faint Companions to Nearby Solar-like Stars using the Adaptive Optics System at Mount Wilson Observatory", The Astronomical Journal **121**, 6, 3254 (2001).

Vogt, S. S., S. L. Allen, B. C. Bigelow, L. Bresee, B. Brown, T. Cantrall, A. Conrad, M. Couture, C. Delaney, H. W. Epps, D. Hilyard, D. F. Hilyard, E. Horn, N. Jern, D. Kanto, M. J. Keane, R. I. Kibrick, J. W. Lewis, J. Osborne, G. H. Pardeilhan, T. Pfister, T. Ricketts, L. B. Robinson, R. J. Stover, D. Tucker, J. Ward and M. Z. Wei, "HIRES: the high-resolution echelle spectrometer on the Keck 10-m Telescope", Proc. SPIE Instrumentation in Astronomy VIII **2198**, 362 (1994).

Wittenmyer, R. A., M. Endl, W. D. Cochran, A. P. Hatzes, G. A. H. Walker, S. L. S. Yang and D. B. Paulson, "Detection Limits from the McDonald Observatory Planet Search Program", arXiv.org , 1, 177–188 (2006).

Worrall, G., "Can Astrophysical Abundances be Taken Seriously ?", Nature **236**, 5, 15–18 (1972).

Young, P. A., K. Liebst and M. Pagano, "The Impact of Stellar Abundance Variations on Stellar Habitable Zone Evolution", The Astrophysical Journal Letters **755**, 2, L31 (2012).

Zsom, A., Z. Sándor and C. P. Dullemond, "The first stages of planet formation in binary systems: how far can dust coagulation proceed?", Astronomy and Astrophysics **527**, A10 (2011).

APPENDIX A

LINELISTS

Iron Linelist

Wavelength	Ionization state	Lower Ex. Pot.	Log(Osc. St.)	EQWsolar
5,247.06	26	$9 \cdot 10^{-2}$	−4.94	67.6
5,358.12	26	3.3	−3.16	10.2
5,412.79	26	4.44	−1.71	20.1
5,522.45	26	4.21	−1.55	37.5
5,539.28	26	3.64	−2.66	17.4
5,543.94	26	4.22	−1.14	65.2
5,546.5	26	4.37	−1.31	51.2
5,546.99	26	4.22	−1.91	24.3
5,560.21	26	4.43	−1.19	52.1
5,577.03	26	5.03	−1.55	9.7
5,579.34	26	4.23	−2.4	10.3
5,651.47	26	4.47	−2	20.7
5,652.32	26	4.26	−1.95	23.2
5,653.87	26	4.39	−1.64	40
5,667.52	26	4.18	−1.58	51.8
5,679.02	26	4.65	−0.92	58.9
5,731.76	26	4.26	−1.3	57.2
5,732.28	26	4.99	−1.56	14.2
5,741.85	26	4.26	−1.85	34.7
5,752.03	26	4.55	−1.18	54.5
5,775.08	26	4.22	−1.3	53.6
5,778.45	26	2.59	−3.48	17.7
5,784.66	26	3.4	−2.53	27.8
5,809.22	26	3.88	−1.61	50.8
5,852.23	26	4.55	−1.17	41.1
5,855.09	26	4.61	−1.48	22.2
5,856.1	26	4.29	−1.56	33.7
5,858.79	26	4.22	−2.18	13
5,902.47	26	4.59	−1.81	10.3
5,905.67	26	4.65	−0.73	54.2
5,927.79	26	4.65	−1.09	41.8
5,929.67	26	4.55	−1.41	38.4
6,005.54	26	2.59	−3.6	21.2
6,027.05	26	4.08	−1.09	63.8
6,079	26	4.65	−1.12	42.9
6,085.26	26	2.76	−3.1	41.4
6,105.13	26	4.55	−2.05	13.2
6,127.91	26	4.14	−1.4	46.6
6,151.62	26	2.18	−3.3	47.4
6,157.73	26	4.08	−1.26	56.1
6,159.37	26	4.61	−1.97	11.9
6,165.36	26	4.14	−1.47	40.1
6,180.21	26	2.73	−2.78	55.1
6,187.99	26	3.94	−1.72	48.8
6,220.78	26	3.88	−2.46	18.7

6,226.73	26	3.88	−2.22	26.4
6,229.23	26	2.85	−2.97	33.9
6,240.65	26	2.22	−3.23	44.2
6,271.28	26	3.33	−2.72	27.8
6,293.92	26	4.83	−1.72	13.6
6,380.74	26	4.19	−1.38	46.9
6,494.5	26	4.73	−1.46	45.6
6,498.95	26	0.96	−4.7	42.6
6,518.37	26	2.83	−2.45	58.9
6,581.21	26	1.49	−4.68	20.5
6,597.56	26	4.79	−1.07	41.6
6,608.02	26	2.28	−4.03	16
6,627.54	26	4.55	−1.68	24.4
6,703.57	26	2.76	−3.16	41.2
6,705.1	26	4.61	−1.39	44
6,710.32	26	1.49	−4.88	14.1
6,713.75	26	4.79	−1.52	17.4
6,715.38	26	4.61	−1.64	25
6,716.22	26	4.58	−1.92	15.9
6,725.35	26	4.1	−2.3	15.8
6,726.67	26	4.61	−1.13	47.5
6,733.15	26	4.64	−1.58	24.1
6,739.52	26	1.56	−4.79	13
6,752.72	26	4.64	−1.3	37.3
6,786.86	26	4.19	−2.07	23.4
6,837.01	26	4.59	−1.69	18.3
6,857.25	26	4.08	−2.04	23.4
5,234.62	26.1	3.22	−2.22	83.5
5,425.26	26.1	3.2	−3.16	42.5
5,991.38	26.1	3.15	−3.55	29
6,084.11	26.1	3.2	−3.8	20.2
6,147.74	26.1	3.89	−2.83	72
6,149.25	26.1	3.89	−2.88	34.4
6,238.39	26.1	3.89	−2.75	47.7
6,247.56	26.1	3.89	−2.44	51.9
6,369.46	26.1	2.89	−4.23	16.6
6,416.92	26.1	3.89	−2.88	37.6
6,432.68	26.1	2.89	−3.52	41.7
6,442.95	26.1	5.55	−2.64	6
6,446.4	26.1	6.22	−2.11	3.7
6,456.38	26.1	3.9	−2.07	61.5
7,479.7	26.1	3.89	−3.53	9.2
7,515.84	26.1	3.9	−3.42	12.6

Other Elements

Wavelength	Ionization state	Lower Ex. Pot.	Log(Osc. St.)	EQWsolar
4,523.08	58.1	0.51	$4 \cdot 10^{-2}$	14.4
4,607.34	38	0	0.28	46.9
4,628.16	58.1	0.52	0.23	20.3
4,730.04	12	4.34	−2.39	76.8
4,773.96	58.1	0.92	0.25	10.5
4,810.54	30	4.08	−0.17	90.8
4,854.87	39.1	0.99	$-1 \cdot 10^{-2}$	16.1
4,900.12	39.1	1.03	$-9 \cdot 10^{-2}$	57.4
5,024.85	22	0.82	−0.56	73.2
5,052.15	6	7.68	−1.3	37.8
5,082.35	28	3.66	−0.59	69.1
5,087.43	39.1	1.08	−0.17	48.6
5,088.54	28	3.85	−1.04	33.6
5,088.96	28	3.68	−1.24	31.3
5,092.8	60.1	0.38	−0.65	7.6
5,094.42	28	3.83	−1.07	32.6
5,105.55	29	1.52	−1.52	90.8
5,112.28	40.1	1.66	−0.59	9.7
5,113.45	22	1.44	−0.73	27.6
5,115.4	28	3.83	−0.28	79.2
5,200.42	39.1	0.99	−0.49	39
5,218.21	29	3.82	0.47	55.6
5,219.71	22	$2 \cdot 10^{-2}$	−2.24	29.1
5,220.09	29	3.82	−0.45	16.1
5,300.75	24	0.98	−2.13	62.2
5,304.18	24	3.46	−0.69	20.1
5,305.87	24.1	3.83	−1.97	26.7
5,308.42	24.1	4.07	−1.82	26.9
5,311.63	72	1.78	0.13	4.4
5,318.36	21.1	1.36	−2	13.2
5,319.82	60.1	0.55	−0.28	11.7
5,342.71	27	4.02	0.54	32.7
5,352.05	27	3.58	$6 \cdot 10^{-2}$	26.5
5,380.32	6	7.68	−1.61	21.9
5,394.67	25	0	−3.5	81.1
5,420.36	25	2.14	−1.46	87.1
5,473.39	39.1	1.74	−0.83	9.4
5,570.39	42	1.33	0.43	9.6
5,690.43	14	4.93	−1.77	52.6
5,711.09	12	4.35	−1.83	104.1
5,727.06	23	1.08	$-1 \cdot 10^{-2}$	39.6
5,783.09	24	3.32	−0.5	31.2
5,783.89	24	3.32	−0.29	45.8
5,787.93	24	3.32	$-8 \cdot 10^{-2}$	47.4
5,793.08	14	4.93	−2.06	44.9

5,847.01	28	1.68	-3.41	23.2
5,853.69	56.1	0.6	-1	66.7
5,866.46	22	1.07	-0.76	48.7
5,867.57	20	2.93	-1.57	25.2
5,978.54	22	1.87	-0.5	21.7
6,013.53	25	3.07	-0.25	78.7
6,016.67	25	3.08	-0.1	93.6
6,039.74	23	1.06	-0.65	13.2
6,046.02	16	7.87	-0.51	17.1
6,064.63	22	1.05	-1.94	10.1
6,086.28	28	4.26	-0.51	37.9
6,090.22	23	1.08	$-6 \cdot 10^{-2}$	34
6,091.18	22	2.27	-0.37	15.3
6,111.08	28	4.09	-0.81	35.8
6,111.65	23	1.04	-0.71	11.7
6,125.03	14	5.61	-1.51	33.8
6,126.22	22	1.07	-1.43	23.2
6,130.14	28	4.27	-0.94	22.4
6,141.73	56.1	0.7	$-7 \cdot 10^{-2}$	132.8
6,142.48	14	5.62	-1.54	36.8
6,145.01	14	5.62	-1.36	40.3
6,154.23	11	2.1	-1.53	39.8
6,155.13	14	5.62	-0.78	81.4
6,156.8	8	10.7	-0.43	4.1
6,160.75	11	2.1	-1.23	58.4
6,161.3	20	2.52	-1.27	59.8
6,166.44	20	2.52	-1.14	72.3
6,169.04	20	2.52	-0.79	104.1
6,169.56	20	2.53	-0.47	106.7
6,175.37	28	4.09	-0.53	50.5
6,176.8	28	4.09	-0.53	67.3
6,177.25	28	1.82	-3.51	15.2
6,204.61	28	4.09	-1.11	22.8
6,244.48	14	5.61	-1.36	48.4
6,245.62	21.1	1.51	-1.02	36.2
6,251.83	23	0.29	-1.34	16.1
6,258.1	22	1.44	-0.35	52.3
6,261.1	22	1.43	-0.48	46.8
6,318.72	12	5.11	-1.99	39.8
6,320.42	57	0.17	-1.39	5.2
6,327.6	28	1.68	-3.23	40
6,336.1	22	1.44	-1.74	7.8
6,362.35	30	5.79	0.14	55.6
6,363.79	8	0	-9.72	4.9
6,378.26	28	4.15	-1	33.1
6,390.49	57	0.32	-1.47	3.2
6,414.59	28	4.15	-1.18	16.2

6,455	27	3.63	−0.24	16.2
6,455.6	20	2.52	−1.5	58.7
6,471.66	20	2.53	−0.59	85.2
6,482.81	28	1.93	−2.97	40.7
6,491.56	22.1	2.06	−1.79	36.8
6,496.91	56.1	0.6	−0.41	112.2
6,499.65	20	2.52	−0.59	79.8
6,506.35	40	0.63	−0.64	2.5
6,532.88	28	1.93	−3.47	17.9
6,572.8	20	0	−4.28	33.2
6,587.62	6	8.54	−1	14
6,598.61	28	4.23	−1.02	21
6,604.6	21.1	1.36	−1.3	37.1
6,606.95	22.1	2.06	−2.79	6.9
6,635.14	28	4.42	−0.82	19.2
6,643.64	28	1.68	−2.01	101.4
6,645.13	63.1	1.38	0.2	5.6
6,696.03	13	3.14	−1.58	38.1
6,698.67	13	3.14	−1.95	21.9
6,721.86	14	5.86	−0.94	49.1
6,757.17	16	7.87	−0.31	17
6,767.78	28	1.83	−1.89	70.1
6,772.32	28	3.66	−0.98	50.9
6,842.04	28	3.66	−1.48	25.8
7,113.17	6	8.65	−0.77	22.7
7,115.17	6	8.64	−0.93	26.7
7,116.96	6	8.65	−0.91	18.5
7,138.91	22	1.44	−1.7	3.8
7,357.73	22	1.44	−1.12	27
7,468.27	7	10.3	−0.19	4.1
7,657.61	12	5.11	−1.28	103.1
7,698.98	19	0	−0.17	166.2
7,771.94	8	9.15	0.37	79.9
7,774.17	8	9.15	0.22	65.7
7,775.39	8	9.15	0	49.6
7,835.31	13	4.02	−0.47	47.6
7,836.13	13	4.02	−0.31	61.7